

CROSS WAVELET ANALYSIS OF CEREBRAL HEMODYNAMICS IN YOUNG AND
OLDER ADULTS

by

MRUNMAYEE SUNIL GANDHI

Presented to the Faculty of the Graduate School of
The University of Texas at Arlington in Partial Fulfillment
of the Requirements
for the Degree of

MASTER OF SCIENCE IN BIOMEDICAL ENGINEERING

THE UNIVERSITY OF TEXAS AT ARLINGTON

August 2014

Copyright © by Mrunmayee Sunil Gandhi 2014

All Rights Reserved



Acknowledgements

I would like to take this opportunity to express my sincere gratitude to all those people who helped me throughout my thesis work.

First, I would like to thank my thesis advisor Dr. Hanli Liu. This work would have not been possible without her constant mentoring, advice, encouragement, exchange of ideas and discussions throughout the project. I am immensely grateful for her constant support and assistance in the preparation of this thesis.

I would like to thank Dr. Rong Zhang, for his insight and faith were valuable in this work. I am thankful to him for deciding the goal of this thesis and also making me understand the physiology behind this work.

I am very grateful to the members of my thesis committee, Dr. Hanli Liu, Dr. Rong Zhang and Dr. Lina Chalak, for their time and effort.

I would like to thank my colleague, Venkaiah Kavuri PhD, who contributed immensely in my research work. I would also like to thank my friends that I have met along the way; they keep me on track and focused on my goals.

Finally, I am greatly indebted to my parents, Netra and Sunil Gandhi, whose love and support has always encouraged me to pursue my ideas. For me they are an institution of love and inspiration.

August 05, 2014

Abstract

CROSS WAVELET ANALYSIS OF CEREBRAL HEMODYNAMICS IN YOUNG AND
OLDER ADULTS

Mrunmayee Gandhi, MS

The University of Texas at Arlington, 2014

Supervising Professor: Hanli Liu

Measurement of cerebral autoregulation is important for the evaluation of a number of clinical disorders that affect cerebral blood flow. Cerebral autoregulation is a mechanism that involves dilation and constriction in arterioles to maintain relatively stable cerebral blood flow in response to changes of systemic blood pressure. Traditional assessments of autoregulation focus on the changes of cerebral blood flow velocity in response to large blood pressure fluctuations induced by interventions. This approach is not feasible for patients with impaired autoregulation or cardiovascular regulation. Therefore in this thesis, a non-stationary time-frequency analysis method, Cross Wavelet Transform is used, which assess autoregulation by nonlinear phase interactions between spontaneous oscillations at resting state and induced oscillations during repeated sit-stand activity in cerebral hemodynamic variables and blood pressure.

In ten healthy young (22–28 years) and ten healthy older adults (70–80 years), blood pressure was continuously measured in the finger by photoplethysmography, cerebral blood flow velocity was measured in the middle cerebral artery (transcranial Doppler ultrasonography) and cerebral cortical oxygenated hemoglobin (HbO) was also measured using fNIRS, during 5 min resting state and again during repeated sit-stand maneuvers at 0.05 Hz. Cross wavelet phase and coherence was calculated between

young and older subjects during resting state and during repeated sit-stand activity for BP vs., TCD and TCD vs. HbO at very-low-frequency oscillations (0.045–0.055 Hz), low-frequency oscillations (0.09–0.11 Hz) and high-frequency oscillations (0.2–0.3 Hz).

It is observed that, the magnitude of oscillations increased during repeated sit-stand activity as compared to baseline oscillations in both young and older adults. These large magnitude oscillations led to an increase in wavelet coherence compared with spontaneous oscillations (baseline) from 0.48 to 0.96 for repeated sit-stand activity at 0.05 Hz ($p < 0.05$), allowing for more confident assessment of cerebral autoregulation through cross wavelet phase analysis.

Cross wavelet analysis indicated that the relationship between BP and cerebral hemodynamic oscillations does not change under influence of age and physical load. There is no significant statistical difference between young and older subjects during baseline and also during repeated sit-stand activity for BP and hemodynamic variables. The results in this thesis suggest aging-related changes in the microvasculature such as declined spontaneous activity in micro vascular smooth muscle cells and vessel stiffness. Moreover, our results indicate that in addition to local vasoregulatory processes, systemic processes also influence cerebral hemodynamic signals. It is therefore crucial to take the factors of age and BP into consideration for the analysis and interpretation of cerebral hemodynamic data.

This study aims to assess the relationship between BP vs. TCD and TCD vs. HbO during spontaneous oscillations and during repeated sit-stand oscillations in healthy young and elderly subjects cross wavelet phase and coherence analysis.

Table of Contents

Acknowledgements	iii
Abstract	iv
List of Illustrations	viii
List of Tables	xi
Chapter 1 Introduction.....	1
1.1 Clinical Framework	1
1.2 Cerebral Autoregulation.....	3
1.3 Wavelet Transform	6
1.3.1 Non-Stationary Signal Analysis: Time-Frequency Analysis	7
1.4 Organization of this Thesis	11
Chapter 2 Materials and Methods.....	12
2.1 Subjects	12
2.2 Ethical Approval.....	13
2.3 Instrumentation	13
2.4 Experimental Procedures	15
2.5 Data Processing and Analysis.....	16
Chapter 3 Results	22
3.1 Raw Data Analysis.....	22
3.2 Phase and Coherence using Cross Wavelet Analysis	25
3.2.1. Baseline	26
3.2.2. Repeated Sit-Stand Maneuvers	30
3.3 Spectral Power at Baseline and Sit-Stand Maneuvers Oscillations	34
Chapter 4 Discussion	38
4.1 Wavelet Phase and Coherence.....	42

4.1.1 BP vs. TCD dynamic relationship on young and older subjects.	42
4.1.2 TCD vs. HbO dynamic relationship on young and older subjects.....	44
4.2 Conclusion	46
Appendix A Circular Statistics.....	48
Circular Mean and Circular Statistics	49
Appendix B Relation of TCD and BP with TOI.....	51
Wavelet Phase and Coherence for TCD-TOI oscillations	52
References.....	53
Biographical Information	58

List of Illustrations

Figure 1-1 Cerebral autoregulation plateau. 4

Figure 1-2 Time-frequency plane corresponding to STFT 8

Figure 1-3 Coverage of time-frequency surface using wavelets. Higher frequencies are analyzed with better time resolution, and lower frequency resolution, while lower frequencies analysis is performed at higher frequency resolution, but lower time resolution..... 9

Figure 2-1 Schematic of the experimental protocol. The figure shows the two sections of the study. Baseline and repeated Sit-stand activity. 16

Figure 2-2 Raw data before using first order polynomial fit (sgolay filter) and after using sgolay filter. 17

Figure 2-3 Representation of wavelet coherence transform used for data analysis. 18

Figure 3-1 Beat-to-beat time series of mean TCD, BP and HbO from a representative young subject during resting state (280s) and repeated sit-stand activity (10s-sit and 10s-stand) for 280s . The line in between of the panel marks the starting of sit-stand activity. Note that for repeated sit-stand activity in young subjects there are high magnitude oscillations..... 22

Figure 3-2 Beat-to-beat time series of mean TCD, BP and HbO from a representative an elder subject during resting state (280s) and repeated sit-stand activity (10s-sit and 10s-stand) for 280s . The line in between of the panel marks the starting of sit-stand activity. Note that for repeated sit-stand activity in elder subject there are high magnitude oscillations..... 23

Figure 3-3 Effects of the repeated sit-stand maneuvers on mean blood pressure (BP-green) and cerebral blood flow velocity (TCD-blue). Raw waveform data from a representative individual (young and senior) during repeated sit-stand maneuvers at 0.05

Hz (10-s sit, 10-s stand) is shown. The graph starts with resting state 280s followed by sit-stand activity, leading to increase in BP (green) and TCD (blue). A total of 560s is displayed, showing 14 cycles of the sit-stand maneuvers. Note that despite strong hemodynamic effects, there is no distortion of waveforms. 24

Figure 3-4 Cross wavelet analysis for BP vs. TCD for young (left) and elder subject (right) during baseline. 26

Figure 3-5 Group average bar plots of Wavelet phase (top) and coherence (bottom) in the frequency ranges of VLF, LF, and HF during baseline for Blood Pressure and TCD for young (red) and older (blue) subjects. (* p<0.07, **p<0.05, p<0.005) 27

Figure 3-6 Cross wavelet analysis for TCD vs. HbO for young (left) and elder subject (right) during baseline..... 28

Figure 3-7 Group average bar plots of Wavelet phase (top) and coherence (bottom) in the frequency ranges of VLF, LF, and HF during baseline for TCD and Oxy-hemoglobin (HbO) for young (red) and older (blue) subjects. (* p<0.07, **p<0.05, p<0.005) 28

Figure 3-8 Cross wavelet analysis for BP vs. TCD for young (left) and elder subject (right) during repeated sit-stand activity. 30

Figure 3-9 Group average bar plots of Wavelet phase (top) and coherence (bottom) in the frequency ranges of VLF, LF, and HF during repeated sit-stand activity for Blood Pressure and TCD for young (red) and older (blue) subjects. (* p<0.07, **p<0.05, p<0.005) 31

Figure 3-10 Cross wavelet analysis for TCD vs. HbO for young (left) and elder subject (right) during repeated sit-stand activity..... 32

Figure 3-11 Group average bar plots of Wavelet phase (top) and coherence (bottom) in the frequency ranges of VLF, LF, and HF during repeated sit-stand activity for TCD and

Oxy-hemoglobin (HbO) for young (red) and older (blue) subjects. (* $p < 0.07$, ** $p < 0.05$, $p < 0.005$) 33

Figure 3-12 Wavelet spectral power at VLF range (0.045-0.55Hz) for TCD, BP, HbO and Hb for young and elder subjects during repeated sits-stand and baseline oscillations. ... 35

Figure 3-13 Wavelet spectral power at LF range (0.09-0.11Hz) for TCD, BP, HbO and Hb for young and elder subjects during repeated sits-stand and baseline oscillations..... 35

Figure 3-14 Wavelet spectral power at HF range (0.2-0.3Hz) for TCD, BP, HbO and Hb for young and elder subjects during repeated sits-stand and baseline oscillations..... 36

List of Tables

Table 2-1: Subject Characteristics and hemodynamics. Values are presented as means and standard deviations.	13
Table 3-1 shows that the mean values of BP and TCD	25
Table 3-2 Wavelet phase for BP vs. TCD and TCD vs. HbO for young and older adults during baseline.	36
Table 3-3 Wavelet phase for BP vs. TCD and TCD vs. HbO for young and older adults during repeated sit-stand activity	37
Table 3-4 Wavelet coherence for BP vs. TCD and TCD vs. HbO for young and older adults during baseline oscillations.	37
Table 3-5 Wavelet coherence for BP vs. TCD and TCD vs. HbO for young and older adults during repeated sit-stand activity.....	37

Chapter 1

Introduction

In this chapter, the principal concepts treated in this thesis are introduced. This chapter will define the clinical and methodological framework for the development of this thesis. In section 1.1, the basis about cerebral hemodynamics and its clinical importance are discussed. In section 1.2, the concept of cerebral autoregulation (CA) and its importance in cerebral hemodynamics monitoring are introduced. In section 1.3 the wavelet transform is introduced, as well as its importance for the time-frequency analysis of signals has been discussed and then the chapter will end with a discussion of the main goals in this thesis and section 1.4 includes an overview of the thesis.

1.1 Clinical Framework

One of the most important causes of brain injury is disturbances in cerebral hemodynamics. In older adults, brain injury might lead to mental and motor disabilities [1,2]. Therefore, monitoring cerebral hemodynamics is of great importance in this population. Under normal circumstances, the brain is protected from pathological disturbances, and variations of some physiological variables, by a series of homeostatic mechanisms; which keep the CBF (Cerebral Blood Flow) relatively constant. When one or more of these mechanisms are disrupted, the brain is exposed to damage. Studies of cerebral hemodynamics, reported in the literature, quantify the status of these mechanisms by investigating the physiology of CBF and its relation with variations in systemic variables.

Cerebral hemodynamics covers the terms related to the dynamics of cerebral blood flow (CBF), cerebral blood volume (CBV) and cerebral blood flow velocity (CBFV). Cerebral blood flow (CBF) plays a central role in cerebral metabolism since it is responsible for the delivery of nutrients and oxygen to the brain [3]. An adequate CBF

will keep a balance between nutrients delivery and consumption in order to maintain the brain homeostasis, by preserving the brain energy levels through the oxidative metabolism of glucose. Deficit in these levels will result in disturbance or loss in brain function, and, if sustained, can lead to brain damage [4]. Therefore, changes in CBF might be caused by pathological conditions related to a reduction in brain energy levels. However, changes in CBF without knowing the status of oxygen delivery and consumption is of no clinical use, since they cannot be linked to pathological conditions. There are several systemic variables that affect cerebral circulation. First of all, under extreme or pathological conditions, changes in mean arterial blood pressure (MABP) produce changes in CBF. However, under normal circumstances the brain is protected from variations in MABP by the cerebral autoregulation (CA) mechanism. CA (cerebral autoregulation) acts over a wide range of blood pressure values where changes in MABP do not reflect changes in CBF. But, when MABP values are outside this range the CBF starts to follow the dynamics of MABP, under this condition the CBF is said to become pressure passive. The lower and upper bounds where CA is active and is known in adults. Some studies indicate that the lower bound in MABP values might be located around 30mmHg, but no information has been reported for the upper limit [5]. Since low MABP values may cause hypoxia due to a low brain perfusion, while a high MABP might cause hemorrhage due to the rupture of small capillaries, monitoring MABP and its relation with CBF is of vital importance in order to avoid brain damage.

Second, concentration of gases such as CO₂ and O₂ and their partial pressures, pCO₂ and pO₂ respectively, have a high impact on CBF [6,7]. On one hand, increasing values of pO₂ produce a mild vasoconstriction which causes a decrease in CBF. On the other hand, in contrast with pO₂, an increase in pCO₂ values produces vasodilation which increases CBF. The effect of pCO₂ is more pronounced than the effect of pO₂ on

the CBF. Thus the relationship of Oxy-hemoglobin and Deoxy-hemoglobin with (Cerebral Blood Flow Velocity) CBFV and BP are important. By monitoring the relation between systemic changes and cerebral hemodynamics variables pathological conditions can be identified and adequate treatment can be provided in order to avoid brain damage.

In clinical practice, monitoring of cerebral hemodynamics, present several challenges. On one hand, brain homeostasis is maintained by several mechanisms that react to changes in several systemic variables and are highly interrelated. This implies that variations in one of the systemic variables produces a cascade of reactions that will affect the other variables as well [8]. Therefore, the multivariate nature of cerebral hemodynamics should be taken into account in order to identify, accurately, pathological conditions.

1.2 Cerebral Autoregulation

As has been mentioned before, cerebral autoregulation (CA) assessment is a field of high interest due to its high clinical impact. Detection of disruptive cerebral autoregulation (CA) can help to prevent brain damage. However, due to the multivariate (multiple input-multiple output) and nonlinear nature of the underlying mechanisms involved in the regulation of CBF, the physiological pathways responsible for cerebral autoregulation are not yet fully understood [9].

Cerebral Autoregulation (CA) is defined as the property of the brain to regulate the changes in CBF in the presence of changes in MABP. The first approaches to assess the status of CA evaluated the relation between CBF and MABP, by provoking changes in MABP and measuring the response in CBF. Figure 1-1 shows how this relation looks like. In this figure it can be seen that for low or high values of MABP, small changes in MABP produce large variations in CBF. While, for a certain range of values, changes in MABP will produce a mild variation in CBF [10]. It is important to note that in this

autoregulative region, the slope of the relation between MABP and CBF is not zero, revealing a weak linear relation between those variables.

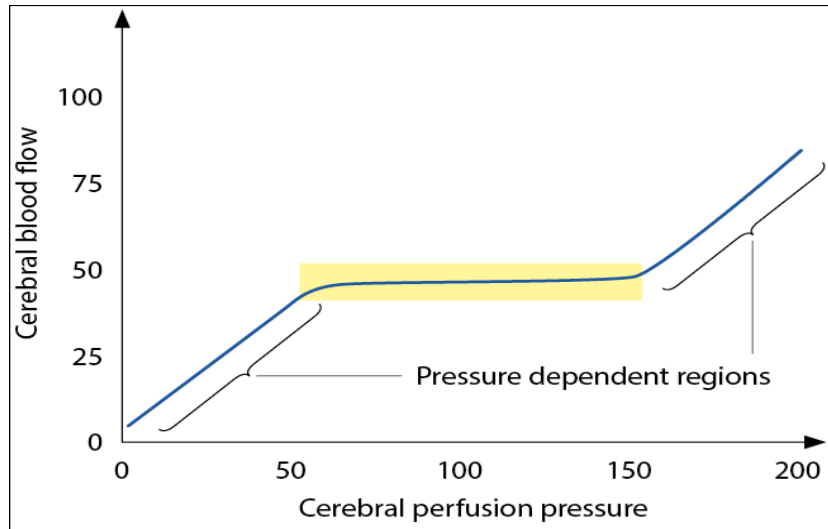


Figure 1-1 Cerebral autoregulation plateau.

Generally, the main limitation in measuring CBF was the difficulty in measuring it continuously. But by the inclusion of new technologies such as transcranial Doppler (TCD), the time resolution of CBF measurements was improved, allowing the study of the transient relations between changes in MABP (mean arterial blood pressure) and CBF [11]. This allows the use of dynamical models to assess the status of cerebral autoregulation. In many contexts correlation, transfer function analysis, coherence, and other methods are used to quantify the status of cerebral autoregulation (CA). However, these models do not take into account the effect of other physiological variables on CA. Recently, it has been suggested that CA is a multivariate process where several mechanisms are involved in its control. Among those the myogenic, metabolic and neurogenic mechanisms have been indicated as the most relevant ones for the regulation of CBF. Recent studies in CA have investigated the influence of pCO₂ on CA [6,7]. However, these influences have been studied as an additive effect using linear models

[11]. In addition, the relation between the different mechanisms regulating CA is not expected to be linear. Thus a multivariate process called as Wavelet Transform is used in this study for analyzing CBF and other hemodynamic variables.

Even though TCD has provided a suitable framework for assessment of CA, its measurements are highly affected by movement artifacts. Near infrared Spectroscopy (NIRS) is a recent technology that has been used to measure hemodynamical variables. NIRS allows the continuous monitoring of changes in oxy- and deoxy-hemoglobin concentration, from which the tissue oxygenation index (TOI) can be computed. TCD studies have shown that the use of a nonlinear multivariate framework improves the assessment of CA. In this context, the cross wavelet analysis is used which can be useful to compute the physiology of the underlying mechanisms that control CBF regulation.

Studies in healthy aging (≥ 75) suggest that the regulation of cerebral blood flow is preserved and that dynamic cerebral autoregulation (dCA) reduce the effects of rapid BP changes [12]. However, data in the aging population are scarce, especially for those over the age of 75. In these older patients, autoregulation studies can contribute valuable clinical information by identifying patients at high risk for cerebral ischemia due to impaired perfusion. To differentiate between health and disease in aging, however, it is essential to be better informed of the influence of normal aging on the behavior of dynamic Cerebral Autoregulation. In this population, it is essential that methods to assess dynamic Cerebral Autoregulation are minimally obtrusive. As such, the dynamic component of cerebral autoregulation is well assessed by beat-to-beat measurements of BP and cerebral blood flow velocity (CBFV), facilitated by Finapres and transcranial Doppler ultrasonography, respectively [11]. Cross wavelet analysis of spontaneous oscillations in BP and CBFV enable the assessment of dynamic Cerebral Autoregulation under resting conditions and, therefore, would seem ideally suited for older subjects.

Repeated sit-stand activity, as used in this study, produces dramatic changes in BP. In daily life comparable maneuvers occur frequently, e.g., when standing up after tying shoelaces or picking up something from the floor, and these maneuvers are often accompanied by symptoms of light-headedness suggestive of cerebral hypoperfusion. When such sit-stand maneuvers are performed repeatedly, large and periodic changes in BP and CBFV are created. Thus, the magnitude of these changes is representative of daily life challenges for cerebral autoregulation [13]. Therefore in this study, relation between, 1. BP and TCD, 2. TCD and HbO have been evaluated during resting state and also during repeated sit-stand maneuvers in young and older adults, for the assessment of cerebral autoregulation.

1.3 Wavelet Transform

In clinical practice several methods are used in order to assess the status of cerebral hemodynamics and cerebral autoregulation. Among all the methods, transfer function is the most commonly used ones. This method represents a univariate (single input-single output) framework for the analysis of the common dynamics between two signals. In the transfer function method, the mean arterial blood pressure (MABP) is used as the “input” while the cerebral blood flow (CBF) is used as output. However, transfer function analysis is generally applied to stationary signals, but when signals are non-stationary i.e. when signals are dependent on time and frequency both, stationary signal analysis like transfer function do not provide accurate results [14].

The oxy-hemoglobin signals consist of notably different features in both time and frequency, of which high-frequency components have a shorter time span than the low-frequency components. A Fourier transformation fails either the following of the time evolution of the high-frequency events or the estimation of the frequency content of the low-frequency band [15]. Therefore, methods in time-frequency domain analysis should

be considered. By this definition, wavelet analysis via the Morlet wavelet can detect various frequency bands in HbO and Hb oscillations with logarithmic frequency resolution [16]. Different characteristic frequencies of HbO signals, which indicate possible regulatory mechanisms of the tissue-oxygenation signal, have been identified using wavelet analysis. Most of the study performed till now, used transfer function analysis but this method is used only for stationery processes, which do not give accurate results. Wavelet transform is used for non-stationery processes which can be used to compute the dynamic relationship between different parameters and also to evaluate cerebral autoregulation. The wavelet transform is explained in detail below.

1.3.1 Non-Stationary Signal Analysis: Time-Frequency Analysis

1.3.1.1 The Short-Time Fourier Transform

The short-time Fourier transform (STFT), first introduced by Gabor(1946), is a Fourier related transform that determines the sinusoidal frequency and phase content of local sections of a signal as it changes over time. It incorporates a degree of time localization into the Fourier transform by applying a moving window function of finite length. As the window sliding along the time axis, the resulting two-dimensional signal can be expressed as:

$$STFT \{x(t)\} = X(f, \tau) = \int_{-\infty}^{\infty} x(t) w(t - \tau) e^{-j2\pi ft} dt \quad 1$$

Where $w(t)$ is the window function, for example, a Gaussian window given by:

$$w(t) = \frac{e^{-t^2/2\sigma^2}}{\sigma\sqrt{2\pi}} \quad 2$$

The parameter σ , defines the width of the window in the time domain. A large value of σ increases the frequency resolution of the estimate, however reduces the

temporal resolution; a small σ would result in good temporal resolution at the cost of a poor frequency resolution. A frequency vs. temporal resolution trade-off exists in the choice of window length, defined by σ here, which is the biggest downfall of the STFT method. Figure 1-2 represents the STFT method, in which its limitations are that, 1. It has a fixed resolution, and 2. Hiesenberg uncertainty principle, which states that at one point of signal, both time and frequency resolution cannot be obtained. Many real signals require good time resolution for high-frequency events, and good frequency resolution for low-frequency events, therefore it is sensible to use a window length that varies depending upon the frequency being analyzed. This is the approach adopted by the wavelet transform (or multi-resolution analysis in general).



Figure 1-2 Time-frequency plane corresponding to STFT

1.3.1.2 The Continuous Wavelet Transform

To overcome the limitation of the STFT, one can imagine letting the resolution of time and frequency vary in the time-frequency plane in order to obtain a multi-resolution analysis. This analysis works best if the signal is composed of high frequency components of short bursts and low frequency components of long duration which is often encountered in practice, especially in biological and medical signals. And this is why the continuous wavelet transform is used for the analysis of the cerebral hemodynamic signals.

Wavelet Transform is a multi-resolution analysis, the time-frequency resolutions of wavelets are different at different positions in the time-frequency surface, unlike what happens with the STFT. Wavelet transform is a mathematical tool that provides an optimal representation of a signal in the time-scale domain. In contrast with Fourier analysis, wavelet provides a framework to study non-stationary signals.

Wavelet is a waveform of effectively limited duration that has an average value of zero. It is a windowing technique with variable-sized regions. Figure 1-3 shows that it has long time intervals where more precise low frequency information is needed and shorter regions where high-frequency information is of interest.

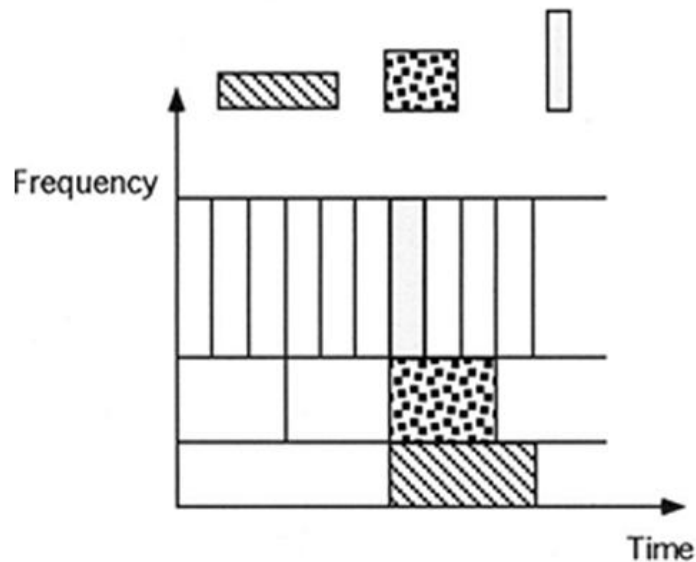


Figure 1-3 Coverage of time-frequency surface using wavelets. Higher frequencies are analyzed with better time resolution, and lower frequency resolution, while lower frequencies analysis is performed at higher frequency resolution, but lower time resolution.

A wavelet is a function with zero mean and that is localized in both frequency and time. The wavelet can be characterized by how localized it is in time (Δt) and frequency

($\Delta\omega$ or the bandwidth). The classical version of the Heisenberg uncertainty principle tells that there is always a tradeoff between localization in time and frequency. One particular wavelet, the Morlet, is defined as

$$\psi_0(\eta) = \pi^{-1/4} e^{i\omega_0\eta} e^{-\eta^2/2} \quad 3$$

where ω_0 is dimensionless frequency and η is dimensionless time. When using wavelets for feature extraction purposes the Morlet wavelet (with $\omega_0=6$) is a good choice, since it provides a good balance between time and frequency localization.

The wavelet phase coherence can reveal possible relationships by evaluating the match between the instantaneous phases of two signals. Cross Wavelet transform identifies high common power, whereas wavelet phase coherence finds locally phase-locked behavior. The wavelet phase coherence analysis has been used to analyze the relationships between oscillations in skin blood flow, temperature, and oxygen saturation within certain frequency ranges [15].

The first aim of this study is to assess the accuracy, reproducibility, and feasibility of repeated sit-stand maneuvers to produce robust and clinically relevant BP and CBFV oscillations and to assess dynamic Cerebral Autoregulation in young and old subjects aged ≥ 70 years and also to assess how CBF changing during sit-stand changes the other parameters. The second aim of this study is to find out the relationship between oscillations in BP, TCD and oxy-hemoglobin (HbO), and to see how they are associated with changes in body posture.

The primary aims of the present study are to characterize age-related differences in cerebral hemodynamics during repeated sit-stand at very low frequency range (0.045-0.55Hz), at low frequency (0.09-0.11Hz) and high frequency (0.2-0.3Hz) in healthy

human subjects and to compute wavelet phase and coherence, to find out the relationship between the cerebral hemodynamic variables (TCD and HbO) and BP.

It is hypothesized that, during repeated sit-stand, the elderly adults have less phase difference BP and CBFV, as at old-age the arteries get stiff and move less efficiently, thus at young age there should be slightly high phase difference than young age. There is high coherence at VLF range, and the gain for all parameters goes on decreasing with increase in frequency for both young and elderly subjects. Thus, there are no significant age-related differences during repeated sit-stand at VLF range.

1.4 Organization of this Thesis

In chapter 2, how the data was collected and methods used to analyze the data have been discussed. The phase and coherence calculation using cross wavelet transform has been discussed in detail in this chapter. Chapter 3 shows the results of the data analysis, this chapter shows how the cross wavelet phase and coherence differ between young and senior subjects during baseline oscillations and during repeated sit-stand activity. Chapter 4 includes discussion on the obtained results and the final physiological conclusion.

Chapter 2

Materials and Methods

2.1 Subjects

Twenty subjects were recruited by the Presbyterian Hospital of Dallas through flyers and newspaper advertisements from the Dallas/Fort Worth metropolitan area. Out of the twenty subjects, ten were elderly subjects (age: 75 ± 3.4 years) and ten were young subjects (age: 24.9 ± 1.85 years). They rigorously screened the subjects using a 12-lead electrocardiogram, 24-hour ambulatory blood pressure, and echocardiogram to exclude cardiovascular disease. They performed Carotid ultrasonography on each subject to exclude individuals with atherosclerotic plaque or stenosis that occluded the common and/or internal carotid artery by $>50\%$. They also checked if any Participants had following criteria: blood pressure ($\geq 140/90$ mm Hg), fasting blood glucose (≥ 126 mg/dL), body mass index (≥ 35 kg/m²), smoking, pregnancy, and the presence or history of cerebrovascular (e.g., stroke), metabolic (e.g., diabetes), neurologic, psychiatric, or inflammatory diseases, brain damage or trauma, hypothyroidism, active alcoholism, or drug abuse. If any Participants meet such conditions those Participants they excluded from the study. Individuals who are taking antihypertensive medications or participating in regular exercise were also excluded for their potential impact on cerebral and central hemodynamics[16].

Prior to the experiment, basic subject information, including age, weight, height, and blood pressure was recorded (table1).

2.2 Ethical Approval

This study was approved by the Institutional Review Board of the University of Texas Southwestern Medical Center and Texas Health Presbyterian Hospital Dallas, and was performed in accordance with the guidelines of the Declaration of Helsinki and Belmont Report. All subjects gave informed written consent before participation [16].

Table 2-1: Subject Characteristics and hemodynamics. Values are presented as means and standard deviations.

Characteristic	Young	Old	t-test P value
Age (years)	24.9	75	
Body mass index (kg/m ²)	23	27	0.02*
Female sex	5	6	
Systolic pr (mmhg)	115.13	124.9	0.14
Diastolic pr (mmhg)	69.25	72.3	0.53
Weight (kg)	63.75	86.11	0.03*
Height (cm)	166.37	185.55	0.98
cfPWV (m/s)	7.17	12.33	0.21
CVRi (mmhg/cm/s)	1.60	1.98	0.08
Vmean (cm/s)	58.40	46.11	0.36
MAP (mmhg)	100.40	86.87	0.35
HR (beats/min)	80.75	71	0.049*

* P values for differences are calculated using t-test for means and standard deviations * <0.05 **<0.05

2.3 Instrumentation

All data was collected, by the Texas Health Presbyterian Hospital Dallas, in an environmentally controlled laboratory with an ambient temperature of 22°C. Subjects were abstained from caffeinated beverages, alcohol, and vigorous exercise for ≥24 hours before the study. After subjects rested in the supine position for ≥10 minutes, intermittent brachial cuff blood pressure was measured at least three times using an ECG-gated electrospigmomanometer (Suntech, Morrisville, NC, USA) and averaged to obtain systolic and diastolic blood pressures. Heart rate was monitored using a 3-lead ECG (Hewlett-Packard, Palo Alto, CA, USA). Middle cerebral artery blood flow velocity was

obtained using a transcranial Doppler (TCD) (Multi-Dop X2; Compumedics/DWL, Singen, Germany) and end-tidal CO₂ was recorded via a capnograph (Capnogard; Novamatrix, Wallingford, CT, USA). All of these variables were continuously recorded throughout data collection. Beat-by-beat blood pressure waveforms from the common carotid, brachial, femoral, and radial arteries were recorded continuously for ≥ 10 seconds using an applanation tonometry (SphygmoCor 8.0; AtCor Medical, West Ryde, NSW, Australia). During the tonometric measurements, they placed a pressure sensor directly on skin and pressed on the arteries at a location where the strongest pulse was felt and the vessel was well supported by an underlying bone structure. Cerebral blood flow velocity (CBFV) was measured over the temporal window on the same side to the carotid pressure measurement using a 2-MHz TCD probe, which was fixated at a constant angle by a probe holder (Spencer Technologies, Seattle, WA, USA). They adjusted the insonation depth and angle to optimize the signal quality and strength according to a standard procedure.¹⁶ End-tidal CO₂ and breathing frequency were monitored by a nasal cannula. During data collection, subjects were instructed to breathe normally and avoid body movement and swallow maneuvers. To ensure stable hemodynamics, intermittent brachial cuff and continuous finger blood pressures (Finapres; Ohmeda, Boulder, CO, USA) were recorded throughout data collection. Arterial blood pressure and CBFV waveforms were inspected visually to obtain high quality signals and to exclude artifacts. Arterial blood pressure and CBFV waveforms were collected with a sampling frequency of 1,000 Hz and analyzed offline using the data analysis software (Acknowledge, BIOPAC Systems, Goleta, CA, USA & DADiSP, Newton, MA, USA). Carotid-femoral (cfPWV) and carotid-radial pulse wave velocities (i.e., measures of central and peripheral arterial stiffness, respectively) and the tonometric indices of carotid pulse wave were

recorded using a standard procedure described in detail elsewhere (SphygmoCor 8.0, AtCor Medical). [17,18]

2.4 Experimental Procedures

All experiments were performed in the morning, at least 2 h after a light breakfast and 12 h after the last caffeinated beverage or alcohol, in a quiet, environmentally controlled laboratory with an ambient temperature of 22°C. After at least 10 min rest in sitting position, 5-min segments of BP and CBFV data were recorded during spontaneous respiration. These data were used for spectral analysis of spontaneous oscillations in BP and CBFV. Next, repeated sit-stand measurements were performed. After careful instruction and practice, participants were coached into performing these repeated sit-stand activity (2-min stand followed by 3-min sit), for 12 min, separated by 45 s of recovery between the baseline and sit-stand activity. Again after careful instruction and practice, participants were coached into performing repeated sit-stand activity at a frequency of 0.05 Hz (10-s sit followed by 10 s standing up), for 5 min, separated by 2 min of recovery between the maneuvers. During these maneuvers, subjects were instructed to keep normal breathing and to avoid a Valsalva-like maneuver. In this study for data analysis, 5 min baseline data followed by repeated sit-stand activity at a frequency of 0.05 Hz (10-s sit followed by 10 s standing up), for 5 min was taken. The middle part of the experiment of repeated sit-stand activity (2-min stand followed by 3-min sit), for 12 min, was excluded. Thus figure (2.1) below shows the protocol taken for the analysis of data.

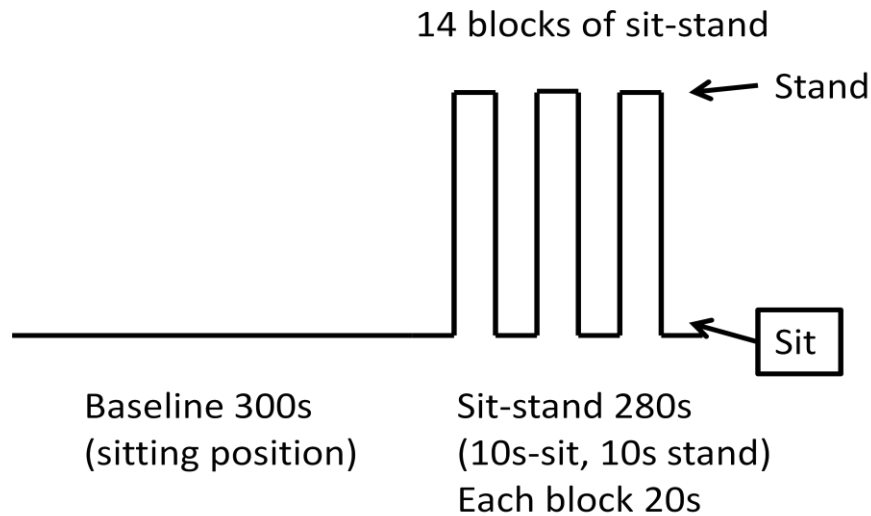


Figure 2-1 Schematic of the experimental protocol. The figure shows the two sections of the study. Baseline and repeated Sit-stand activity.

2.5 Data Processing and Analysis

Steps for processing and analyzing the data are given as follows:

1. BP, ECG and HbO-Hb (oxy and deoxy hemoglobin) were simultaneously recorded at the Texas Health Presbyterian Hospital Dallas with a sample frequency of 1000 Hz. All the data acquired from the Texas Health Presbyterian Hospital Dallas was recorded by the instrument as Acknowledge, BIOPAC Systems, Goleta, CA, USA .
2. The Acknowledge, BIOPAC files were converted into Matlab files and then all the analysis were performed with Matlab (MathWorks, MA, USA).
3. Initially the 1000Hz raw data was down-sampled to 10 Hz in-order to optimize the SNR and resolution of the signal.
4. After down sampling, the data was smoothed by using first order polynomial fit, Savitzky-Golay filter, which tend to filter out a significant portion of the signal's high frequency content along with the noise. These filters are also more effective at preserving

the pertinent high frequency components of the signal. The raw data before and after using this filter is shown in the figure 2-2:

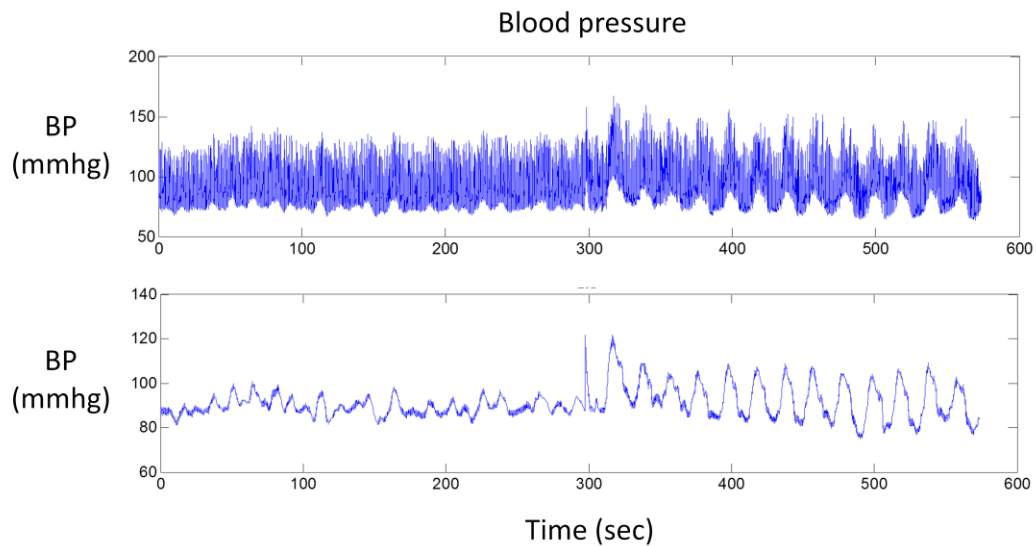


Figure 2-2 Raw data before using first order polynomial fit (sgolay filter) and after using sgolay filter.

5. Then beat-to-beat changes in mean BP, TCD and HbO were aligned with the time of the R wave peaks of the ECG for each subject.

6. The average over entire time period was not taken as it would result into more noise at different frequencies, thus specific time range was selected for sit-stand activity (t= 0:1800s) and baseline (t= 0:2000s) data.

7. Three frequency ranges were selected to perform wavelet transform: 1. Very Low Frequency range (VLF) from 0.045 to 0.055 Hz. 2. Low Frequency range (LF), which originates from fluctuations in sympathetic vasomotor control by the central nervous system, from 0.09 to 0.11 Hz, and 3. High Frequency range (HF) from 0.2 to 0.3 Hz, which originates from fluctuations in cardiac output induced by respiratory movement.

Figure 2-3 shows the three frequency ranges and the color bar showing coherence from 0 (blue- no coherence) to 1 (red- high coherence). The x-axis is the time (sec) and y-axis is frequency (Figure 2-3), the time-axis (0-280s) is divided into fourteen blocks of sit-stand (10s-sit and 10s stand) 20s each block. In Figure 2-3, in the COI (cone of influence) the arrows are present, a rightward arrow indicates 0 lag; a bottom-right arrow indicates a small lead of x; a leftward arrow indicates x and y is anti-correlated.

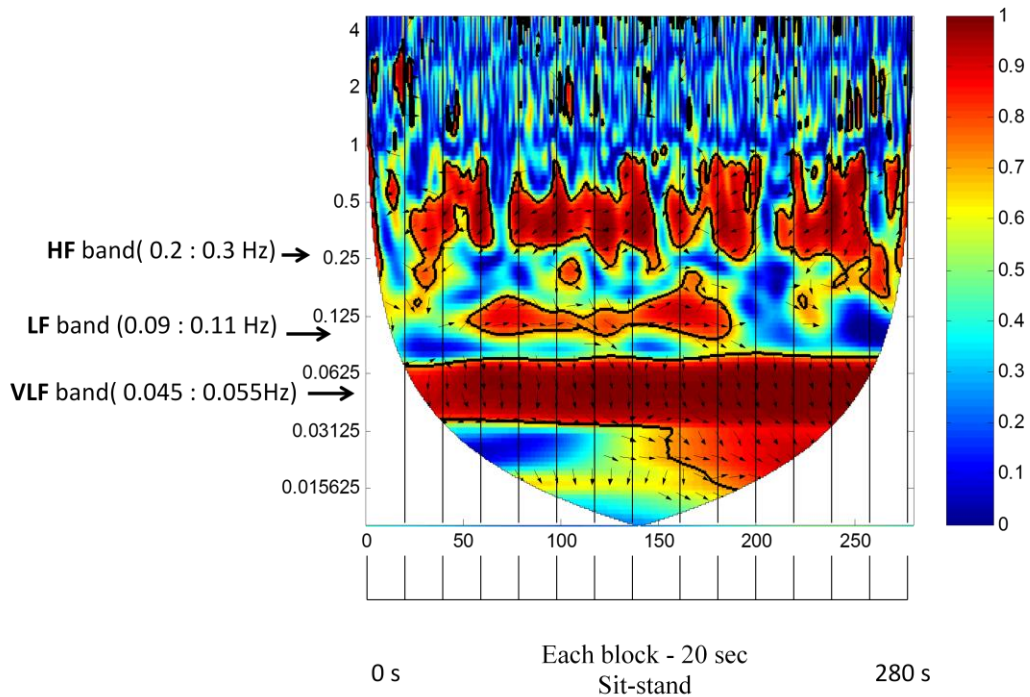


Figure 2-3 Representation of wavelet coherence transform used for data analysis.

8. Then the wavelet transform coherence (wtc) method was used to calculate phase, coherence and power spectrum. For the phase and coherence calculation threshold of 0.4 was used. Above 0.4 coherence threshold, all phases and coherence was calculated for BP vs. TCD and TCD vs. HbO. For the phase and coherence calculation of BP vs. TCD and TCD vs. HbO for all subjects, firstly average across time

for all the data points for individual subject was taken and then average across all young and senior subjects respectively was taken. Then t-test was performed using standard deviation for the analysis between young and older adults.

9. Cross wavelet phase angle and coherence: To quantify the phase relationship between all the parameters (TCD, BP and HbO) the arithmetic mean of the phase over regions with higher than 5% statistical significance was taken. This is a useful and general method for calculating the mean phase. The arithmetic mean of a set of angles ($a_i, i=1\dots n$) is defined as

$$a_m = \arg(X, Y) \quad \text{with} \quad X = \sum_{i=1}^n \cos(a_i) \quad \text{and} \quad Y = \sum_{i=1}^n \sin(a_i) \quad 4$$

10. The wavelet coherence is an extension of the concept of coherence in Fourier analysis. The wavelet coherence values given in (9) produce values equal to one. This is due to the fact that there is no spectral smoothing involved in the computation of the wavelet power spectrum [19,20]. Coherence values computed using the Fourier transform, calculate the cross-power and power spectrum of the signals using the Welch method. This method smoothes the spectrum by computing an average of different realizations of the process under study. When using the wavelet transform, the signal under analysis is considered non-stationary, therefore using the Welch method can produce misleading results. However, by introducing a smoothing operator S, in scale and time, the wavelet spectrum can be smoothed. This operation will reduce the coherence values in segments with no spectral coupling, but will spread the influence of coupled segments in the time-frequency domain.

11. Cross wavelet power reveals areas with high common power. To measure how coherent is the cross wavelet transform is in time frequency space following eq. (9) [19] is used to define the wavelet coherence of two time series as

$$R_n^2(s) = \frac{|\mathcal{S}(s^{-1}W_n^{XY}(s))|^2}{\mathcal{S}(s^{-1}|W_n^X(s)|^2) \cdot \mathcal{S}(s^{-1}|W_n^Y(s)|^2)} \quad 5$$

where \mathcal{S} is a smoothing operator, $W_n^X(s)$ is auto-spectrum of x (input signal) and $W_n^Y(s)$ is auto-spectrum of y (output signal) and $W_n^{XY}(s)$ is cross-spectrum of x and y (i.e. cross-spectrum of two signals). The linearity of the cerebrovascular system is evaluated by this magnitude square coherence function $R_n^2(s)$ (eq. 9). Notice that this definition closely resembles that of a traditional correlation coefficient, and it is useful to think of the wavelet coherence as a localized correlation coefficient in time frequency space. the smoothing operator \mathcal{S} is given as

$$\mathcal{S}(W) = \mathcal{S}_{scale} \left(\mathcal{S}_{time} (W_n(s)) \right) \quad 6$$

where \mathcal{S}_{scale} denotes smoothing along the wavelet scale axis and \mathcal{S}_{time} smoothing in time. For the Morlet wavelet a suitable smoothing operator is given by [21]

$$\mathcal{S}_{time}(W)|_s = \left(W_n(s) * c_1 \frac{-t^2}{2s^2} \right) |_s \quad 7$$

$$\mathcal{S}_{time}(W)|_s = \left(W_n(s) * c_2 \pi(0.6s) \right) |_s$$

Where c_1 and c_2 are normalization constants and π is the rectangle function. The factor of 0.6 is the empirically determined scale decorrelation length for the Morlet wavelet [19]. In practice both convolutions are done discretely and therefore the normalization coefficients are determined numerically.

The wavelet transform phases reflect the relative amplitude and time-frequency relationship between changes in BP and TCD, and also other parameters. Perfect

cerebral autoregulation is represented by a large phase difference between BP and TCD. While impaired cerebral autoregulation produces smaller phase differences, this is an indication of a more pressure passive TCD. When analyzing phase values, phase differences have been focussed at 0.05 Hz and 0.1 Hz since many literature studies have shown the best results at 0.1 Hz which differentiates between impaired and normal autoregulation [22]. There is no physiological explanation for the selection of low-frequency band. However, these results may be related to the Mayer waves. Mayer waves are oscillations of arterial pressure occurring that occur spontaneously at a frequency around 0.1 Hz. They might be generated by oscillations in baroreceptor and chemoreceptor reflex control systems; however, their physiological origin is still unclear. Since spontaneous variations in BP are not strong enough, the influence of the Mayer waves around this frequency might result in an increased signal-to-noise ratio (SNR) for the calculation of the wavelet transform.

Chapter 3

Results

3.1 Raw Data Analysis

Representative changes in BP, TCD, and HbO during baseline, and the 0.05 Hz sit-stand maneuvers, are presented in Figure. 3-1. Note that, HbO oscillations appear clearly related to the oscillations in BP and CBFV. The repeated sit-stand maneuvers induced oscillations in all signals (BP, CBFV, O2Hb), was significantly larger than for baseline oscillations in the VLF, LF and HF range.

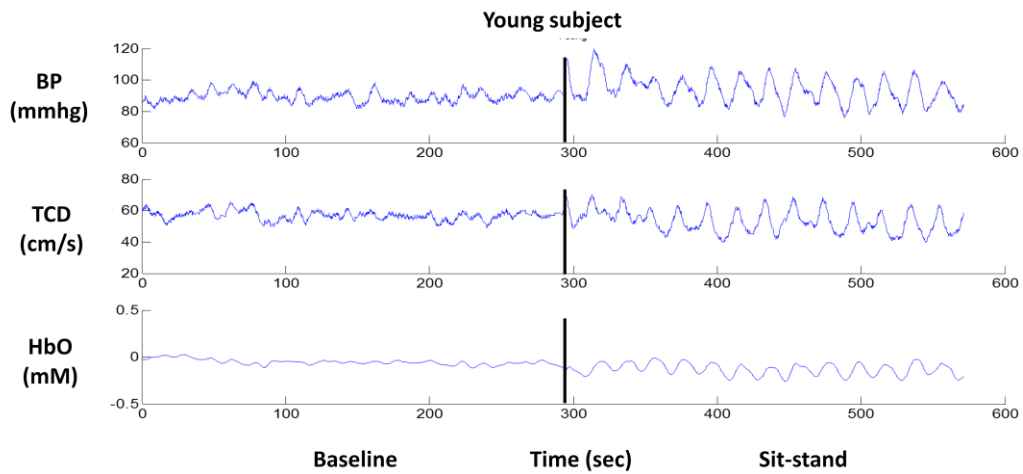


Figure 3-1 Beat-to-beat time series of mean TCD, BP and HbO from a representative young subject during resting state (280s) and repeated sit-stand activity (10s-sit and 10s-stand) for 280s . The line in between of the panel marks the starting of sit-stand activity.

Note that for repeated sit-stand activity in young subjects there are high magnitude oscillations.

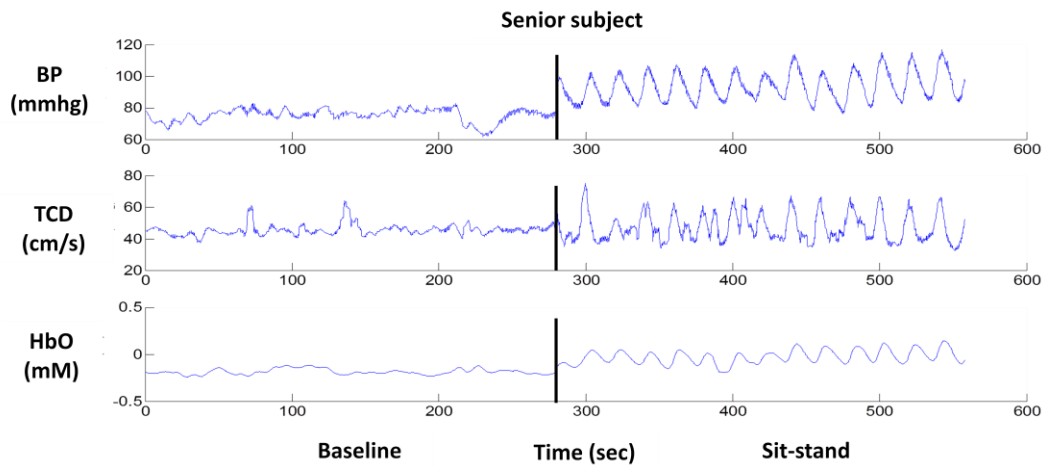


Figure 3-2 Beat-to-beat time series of mean TCD, BP and HbO from a representative an elder subject during resting state (280s) and repeated sit-stand activity (10s-sit and 10s-stand) for 280s . The line in between of the panel marks the starting of sit-stand activity.

Note that for repeated sit-stand activity in elder subject there are high magnitude oscillations.

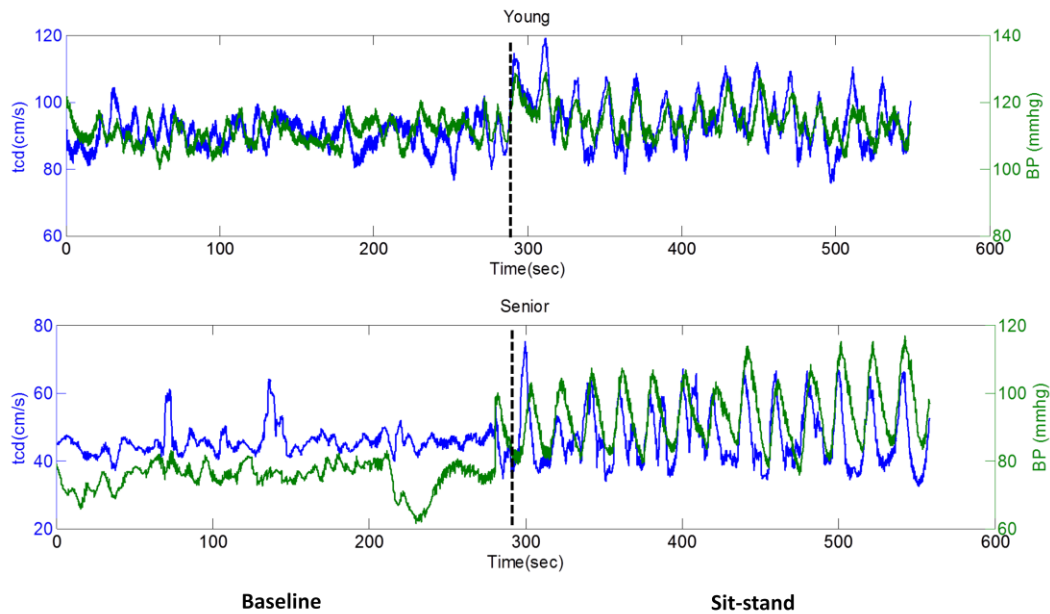


Figure 3-3 Effects of the repeated sit-stand maneuvers on mean blood pressure (BP-green) and cerebral blood flow velocity (TCD-blue). Raw waveform data from a representative individual (young and senior) during repeated sit-stand maneuvers at 0.05 Hz (10-s sit, 10-s stand) is shown. The graph starts with resting state 280s followed by sit-stand activity, leading to increase in BP (green) and TCD (blue). A total of 560s is displayed, showing 14 cycles of the sit-stand maneuvers. Note that despite strong hemodynamic effects, there is no distortion of waveforms.

The resting state, as seen in the figure 3-1, is for 280s and repeated sit-stand activity is for 280s (sit: 10s and stand: 10s - 14 blocks of sit-stand, each block of 20s sit-stand) for both young and older subjects. Large oscillations in BP and TCD are observed at 0.05 Hz during repeated sit-stand maneuvers (Figure 3-1) for both young and older subjects. It is visible from the raw data that TCD oscillations lead BP oscillations (3-2). It is seen below that BP (green) for young subject is going above 120mmhg during

repeated sit-stand activity as compared to older subject which is below 120mmhg. Also TCD (blue) for young subject is varying from 80-100 cm/s, but for older subject it is below 60cm/s.

Table 3-2 shows that the mean values of BP and TCD for young and senior subjects does not change significantly from baseline to the repeated sit-stand maneuvers, despite the increased oscillation amplitude. (These values are for individual young and senior subject).

Table 3-1 shows that the mean values of BP and TCD

Subjects	BP_Baseline (mmhg)	BP_Sit-stand (mmhg)	TCD_Baseline (cm/s)	TCD_Sit-stand (cm/s)
Young	110.71	114.854	90.380	94.805
Elder	75.269	93.527	45.526	47.148

In the above table, for this particular young and older subject, there is significant difference in the raw data BP-TCD baseline and sit-stand values, but when mean is taken of all young and senior subjects for BP-TCD baseline and sit-stand values, there is no such significant difference between them.

3.2 Phase and Coherence using Cross Wavelet Analysis

In this study, Cross-wavelet analysis is used for calculation of phase and coherence between young and elderly subjects at baseline and sit-stand maneuvers at three frequency ranges for BP vs. TCD and TCD vs. HbO. In the literature below is the summarization of the cross wavelet analysis for phase, and coherence in the frequency domains of VLF (0.045:0.055Hz), LF (0.09:0.11Hz), and HF (0.2:0.3Hz) for baseline oscillations and for oscillations by the repeated sit-stand maneuvers for BP vs. TCD and TCD vs. HbO.

3.2.1. Baseline

3.2.1.1 Wavelet phase and coherence for BP vs. TCD oscillations for young and older subjects during baseline.

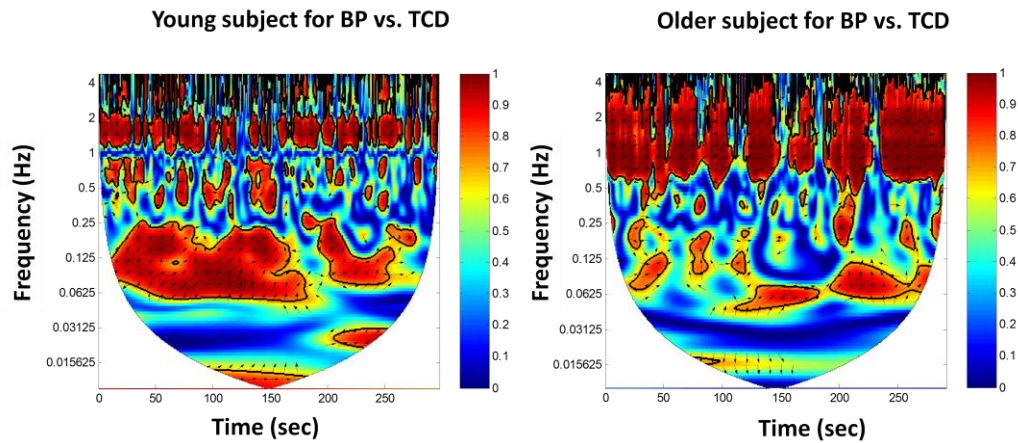


Figure 3-4 Cross wavelet analysis for BP vs. TCD for young (left) and elder subject (right) during baseline.

Figure 3-3 shows the Cross Wavelet analysis for BP Vs.TCD for baseline at VLF, LF and HF for young and elderly subjects. It is seen that for a representative young subject, there is high coherence (red) at LF range (0.09-0.011 Hz) as compared to elder subject during baseline, but for elder subject there is high coherence (red) at HF range (0.2-0.3 Hz). It is also observed in figure 3-3 that in the highly coherent areas the arrows are mostly pointed up, suggesting that TCD is leading BP.

In the Figure 3-4, there is no statistically significant difference between young and elder subjects for phase shift during baseline. Negative phase shift for BP vs. TCD indicates TCD is leading BP. Coherence goes on decreasing from VLF range to HF range. In addition, it is observed that the phase shift goes on decreasing from VLF range (-1.06 ± 0.58) to HF (-0.37 ± 0.17) range for young and VLF range (-0.83 ± 0.48) to HF (-0.37 ± 0.30) range for older subjects during baseline. However, in the high-frequency range, changes in velocity are almost in phase with changes in pressure. In the VLF

range of 0.045–0.3 Hz the coherence was >0.4, suggesting that, in this frequency range, changes in velocity are linearly related to the changes in pressure for baseline measurements. There is statistically significant difference between young and elder subjects during baseline at VLF and LF range (Figure 3-4).

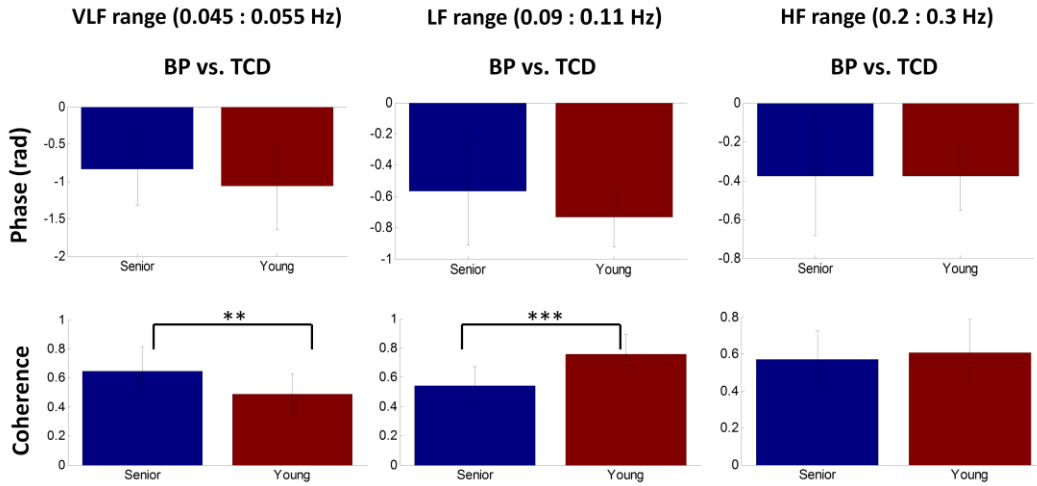


Figure 3-5 Group average bar plots of Wavelet phase (top) and coherence (bottom) in the frequency ranges of VLF, LF, and HF during baseline for Blood Pressure and TCD for young (red) and older (blue) subjects. (* $p < 0.07$, ** $p < 0.05$, *** $p < 0.005$)

3.2.1.2 Wavelet phase and coherence for TCD vs. HbO oscillations for young and older subjects during baseline.

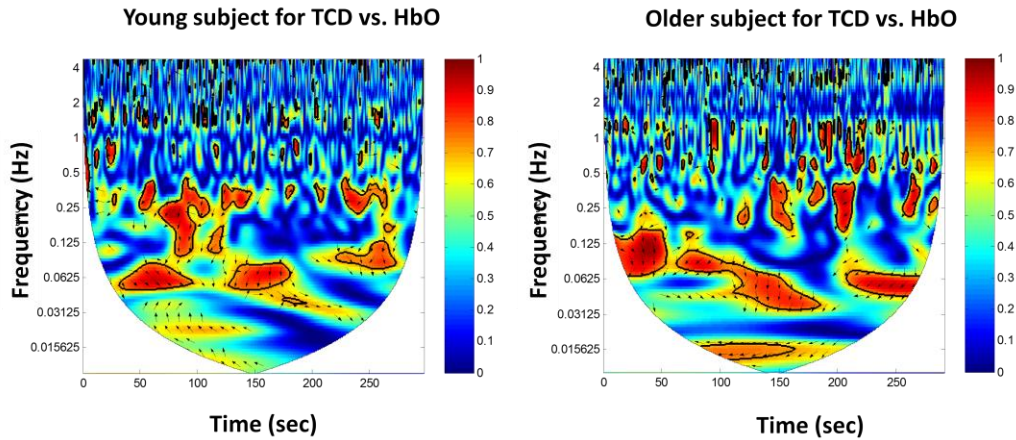


Figure 3-6 Cross wavelet analysis for TCD vs. HbO for young (left) and elder subject (right) during baseline.

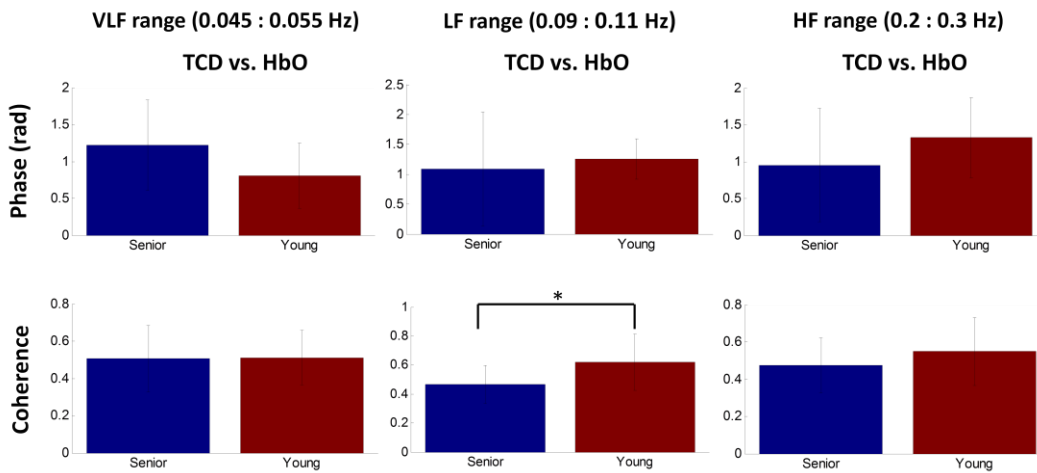


Figure 3-7 Group average bar plots of Wavelet phase (top) and coherence (bottom) in the frequency ranges of VLF, LF, and HF during baseline for TCD and Oxy-hemoglobin (HbO) for young (red) and older (blue) subjects. (* $p < 0.07$, ** $p < 0.05$, $p < 0.005$)

Figure 3-5 shows the Cross Wavelet analysis for TCD vs. HbO for baseline at VLF, LF and HF for young and elderly subjects. It is seen that for a representative young and elder subject, there is very few highly coherent area (red) around LF range (0.09-0.11 Hz). It is also observed in figure 3-5 that in the highly coherent areas the arrows are mostly pointed down, suggesting that TCD is leading HbO.

Figure 3-6 shows the Wavelet phase shift and coherence for TCD vs. HbO during baseline at VLF, LF and HF for young and elderly subjects. It is seen in the figure 3-6, that there is no significant phase shift at VLF, LF and HF range between young and older subjects during baseline for TCD vs. HbO. For young subjects the phase shift for TCD vs. HbO goes on increasing from VLF (0.81 ± 0.44) to HF (1.32 ± 0.54) range, also for elder adults, phase shift is increasing from VLF (1.22 ± 0.61) to HF (1.68 ± 0.76) range. The positive value of phase in the frequency range 0.045-0.3Hz indicates changes in TCD leads changes in Oxy-hemoglobin (HbO). Wavelet coherence is around 0.5 during baseline and shows significant difference between young and older adults during baseline at LF ($p < 0.07$) range.

3.2.2. Repeated Sit-Stand Maneuvers

3.2.2.1 Wavelet phase and coherence for BP vs. TCD oscillations for young and older subjects during repeated sit-stand activity.

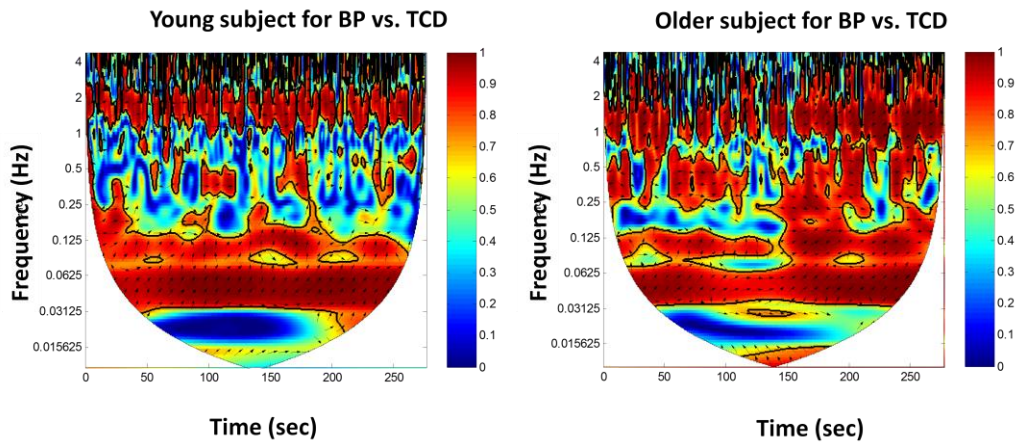


Figure 3-8 Cross wavelet analysis for BP vs. TCD for young (left) and elder subject (right) during repeated sit-stand activity.

Figure 3-7 shows the Cross Wavelet analysis for BP vs. TCD during repeated sit-stand activity at VLF, LF and HF for young and elderly subjects. It is seen that for a representative young and elder subject, there is high coherence (red) at VLF range (0.045-0.055 Hz), LF range (0.09-0.11 Hz) and HF range (0.2-0.3 Hz). This means that TCD and BP are linearly related to each other.

In the Figure 3-8, there is no statistically significant difference between young and elder subjects for phase shift during baseline. Negative phase shift for BP vs. TCD indicates TCD is leading BP. In addition, it is observed that the phase shift goes on increasing from VLF range (-0.86 ± 0.16) to HF (-0.18 ± 0.33) range for young and VLF range (-0.79 ± 0.16) to HF (-0.27 ± 0.30) range for older subjects during repeated sit-stand activity. However, in the high-frequency range, phase shift reaches almost zero for BP vs. TCD, suggesting that TCD depends on BP. In the VLF range of 0.045–0.3 Hz the coherence was >0.4 , suggesting that, in this frequency range, changes in velocity are

linearly related to the changes in pressure during repeated sit-stand activity. There is no statistically significant difference between young and elder subjects during during repeated sit-stand activity. Coherence goes on decreasing from VLF range to HF range.

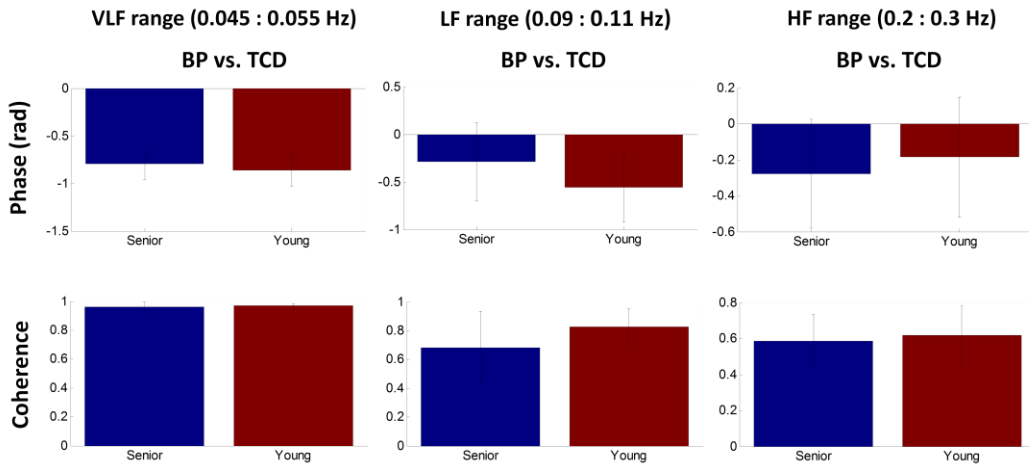


Figure 3-9 Group average bar plots of Wavelet phase (top) and coherence (bottom) in the frequency ranges of VLF, LF, and HF during repeated sit-stand activity for Blood Pressure and TCD for young (red) and older (blue) subjects. (* $p < 0.07$, ** $p < 0.05$, $p < 0.005$)

3.2.2.2 Wavelet phase and coherence for TCD vs. HbO oscillations for young and older subjects during repeated sit-stand activity

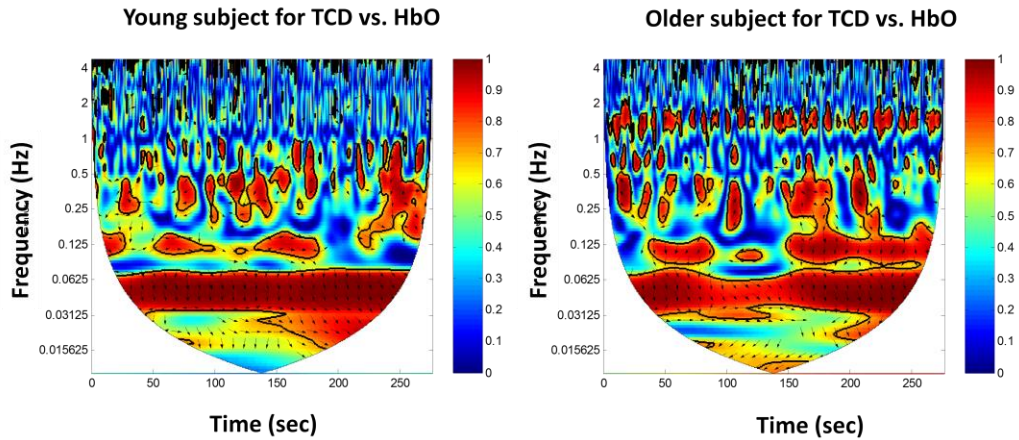


Figure 3-10 Cross wavelet analysis for TCD vs. HbO for young (left) and elder subject (right) during repeated sit-stand activity.

Figure 3-9 shows the Cross Wavelet analysis for TCD vs. HbO during repeated sit-stand activity at VLF, LF and HF for young and elderly subjects. It is seen that for a representative young and elder subject, there is high coherence (red) only at VLF range (0.045-0.055 Hz). The phase arrows in the highly coherent areas are pointing downwards suggesting that TCD leads HbO.

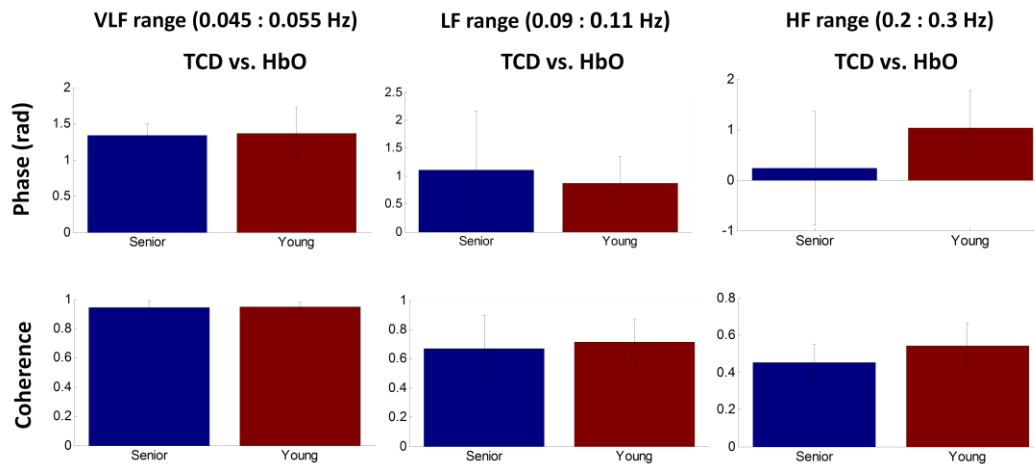


Figure 3-11 Group average bar plots of Wavelet phase (top) and coherence (bottom) in the frequency ranges of VLF, LF, and HF during repeated sit-stand activity for TCD and Oxy-hemoglobin (HbO) for young (red) and older (blue) subjects. (* $p < 0.07$, ** $p < 0.05$, $p < 0.005$)

Figure 3-10 shows the Wavelet phase shift and coherence for TCD vs. HbO during repeated sit-stand activity at VLF, LF and HF for young and elderly subjects. It is seen in the figure 3-10, that there is no significant phase shift at VLF, LF and HF range between young and older subjects during repeated sit-stand activity for TCD vs. HbO. For young subjects, the phase shift for TCD vs. HbO goes on decreasing from VLF (1.36 ± 0.36) to HF (1.04 ± 0.72) range, similarly for elder subjects, the phase shift for TCD vs. HbO goes on decreasing from VLF (1.33 ± 0.16) to HF (0.24 ± 1.12) range. The positive value of phase in the frequency range 0.045-0.3Hz indicates changes in TCD leads changes in Oxy-hemoglobin (HbO). Wavelet coherence is almost 1 (red) during repeated sit-stand activity but shows no significant difference between young and older adults during repeated sit-stand activity.

3.3 Spectral Power at Baseline and Sit-Stand Maneuvers Oscillations

The repeated sit-stand maneuvers at 0.05 Hz resulted in, 2-fold increases in BP spectral power (compared with spontaneous VLF oscillations), while at 0.1 Hz, almost 4-fold increase occurred relative to spontaneous LF oscillations (Figure 3-12). These augmented oscillations in BP led to 1.5-, and 1-fold increases in TCD spectral power at 0.05, and 0.1 Hz, respectively. Thus increases in TCD oscillations were relatively smaller than increases in BP oscillations at 0.05 Hz but not at 0.1 Hz, indicating more effective damping at the lower frequencies (Figure 3-11 and Figure 3-12). For HbO there is 3-fold increase in spectral power during repeated sit-stand maneuvers as compared with spontaneous at VLF oscillations (Figure 3-11), while at LF (Figure 3-12) there is about similar increase spectral power at both during repeated sit-stand maneuvers and during baseline for young and older subjects. But comparatively to young subjects older subjects had less increase in spectral power for HbO.

For HF (Figure 3-13) range there is no significant increase in spectral power between repeated sits-stand and baseline oscillations for young and senior subjects. But for HbO at HF there is increase in spectral power in young subjects as compared to older subjects. Figure 3-11, Figure 3-12 and Figure 3-13 shows the group statistics for the power spectral density analysis at VLF, LF and HF range respectively. The large error bars indicate the variability that is typically encountered in power spectra measured from patients and controls.

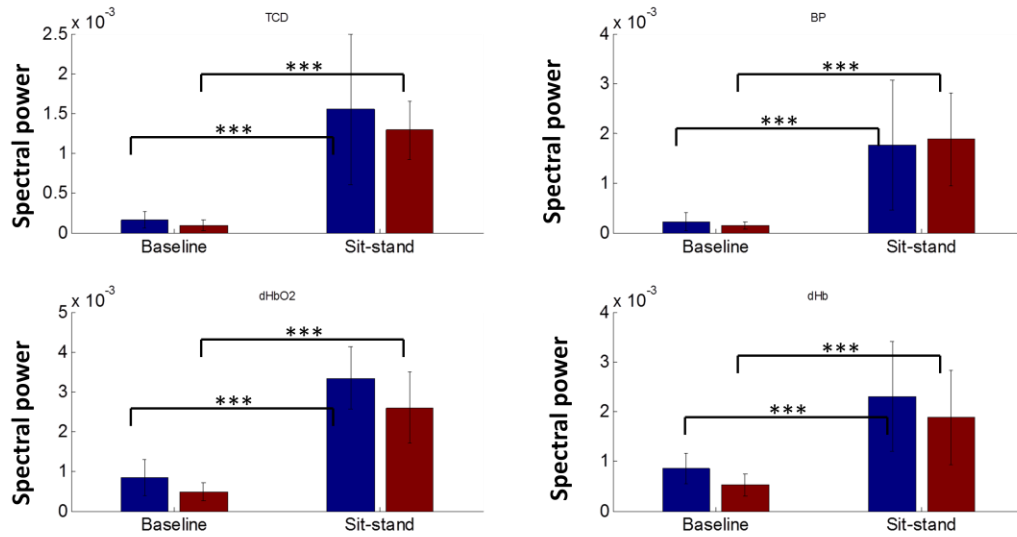


Figure 3-12 Wavelet spectral power at VLF range (0.045-0.55Hz) for TCD, BP, HbO and Hb for young and elder subjects during repeated sits-stand and baseline oscillations.

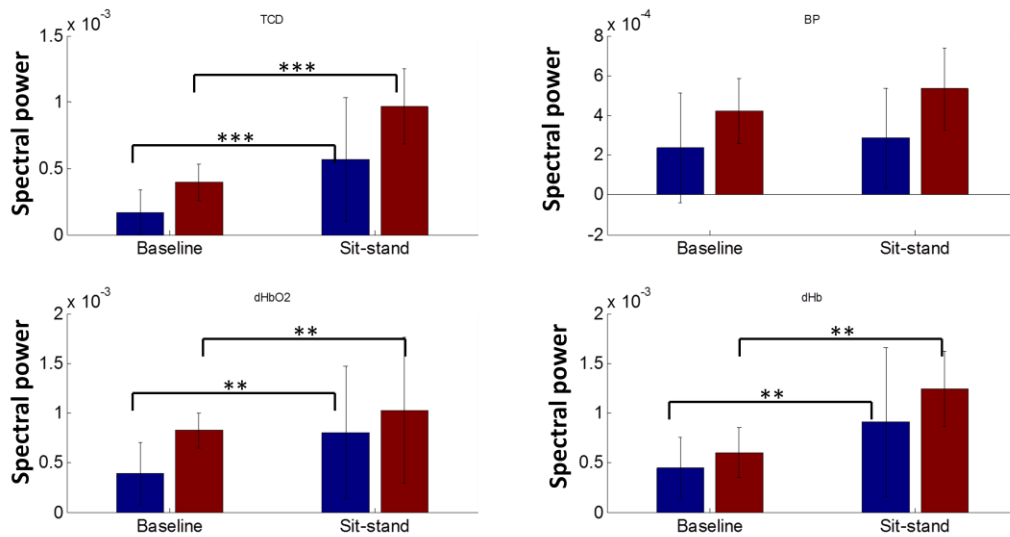


Figure 3-13 Wavelet spectral power at LF range (0.09-0.11Hz) for TCD, BP, HbO and Hb for young and elder subjects during repeated sits-stand and baseline oscillations.

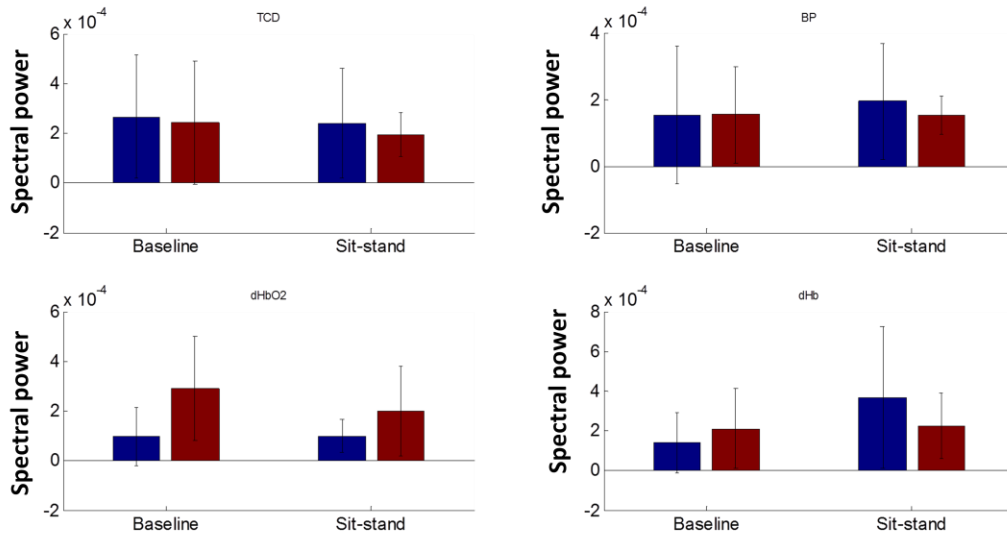


Figure 3-14 Wavelet spectral power at HF range (0.2-0.3Hz) for TCD, BP, HbO and Hb for young and elder subjects during repeated sits-stand and baseline oscillations.

Taken together, the results of Cross Wavelet analysis show a clear relationship between systemic and cerebral oscillations. This relationship displays the known properties of cerebral autoregulation. Below are the tables for BP vs. TCD and TCD vs. HbO for Wavelet phase and coherence during baseline and repeated Sit-stand activity for BP vs TCD and TCD vs HbO.

Table 3-2 Wavelet phase for BP vs. TCD and TCD vs. HbO for young and older adults during baseline.

	Baseline	Young	Elder
Phase			
VLF	BP vs. TCD	- 1.06 ± 0.58	-0.83 ± 0.48
LF	BP vs. TCD	- 0.73 ± 0.18	- 0.56 ± 0.34
HF	BP vs. TCD	- 0.37 ± 0.17	-0.37 ± 0.30
VLF	TCD vs. HbO	0.81 ± 0.44	1.22 ± 0.61
LF	TCD vs. HbO	1.25 ± 0.33	1.08 ± 0.95
HF	TCD vs. HbO	1.32 ± 0.54	1.68 ± 0.76

Table 3-3 Wavelet phase for BP vs. TCD and TCD vs. HbO for young and older adults during repeated sit-stand activity

	Sit-stand	Young	Elder
Phase			
VLF	BP vs. TCD	-0.86 ± 0.16	-0.79 ± 0.16
LF	BP vs. TCD	-0.56 ± 0.36	-0.28 ± 0.41
HF	BP vs. TCD	-0.18 ± 0.33	-0.27 ± 0.30
VLF	TCD vs. HbO	1.36 ± 0.36	1.33 ± 0.16
LF	TCD vs. HbO	0.87 ± 0.47	1.11 ± 1.05
HF	TCD vs. HbO	1.04 ± 0.72	0.24 ± 1.12

Table 3-4 Wavelet coherence for BP vs. TCD and TCD vs. HbO for young and older adults during baseline oscillations.

	Sit-stand	Young	Elder
coherence			
VLF	BP vs. TCD	0.48 ± 0.14	0.64 ± 0.16
LF	BP vs. TCD	0.76 ± 0.13	0.54 ± 0.12
HF	BP vs. TCD	0.61 ± 0.17	0.57 ± 0.15
VLF	TCD vs. HbO	0.51 ± 0.14	0.50 ± 0.17
LF	TCD vs. HbO	0.62 ± 0.19	0.47 ± 0.13
HF	TCD vs. HbO	0.54 ± 0.18	0.47 ± 0.14

Table 3-5 Wavelet coherence for BP vs. TCD and TCD vs. HbO for young and older adults during repeated sit-stand activity

	Sit-stand	Young	Elder
coherence			
VLF	BP vs. TCD	0.96 ± 0.015	0.96 ± 0.03
LF	BP vs. TCD	0.82 ± 0.12	0.68 ± 0.25
HF	BP vs. TCD	0.61 ± 0.16	0.58 ± 0.14
VLF	TCD vs. HbO	0.95 ± 0.02	0.94 ± 0.04
LF	TCD vs. HbO	0.71 ± 0.15	0.67 ± 0.22
HF	TCD vs. HbO	0.54 ± 0.12	0.45 ± 0.09

Chapter 4

Discussion

The aim of this study is to examine interaction effects of age and physical load (repeated sit-stand activity) on VLFOs (0.045–0.055 Hz), LFOs (0.09–0.11 Hz), and HFOs (0.2–0.3 Hz) of cerebral hemodynamics variables (i.e. CBFV and HbO) and BP. This study shows that VLFOs, LFOs, and HFOs of cerebral hemodynamics declined with aging. Cross Wavelet analysis identified a relationship between BP-TCD and TCD-HbO oscillations during a physical load for both young and older adults. Furthermore, it demonstrated that this relationship did not change under influence of age or physical load.

There are several new findings in this study. During repeated sit-stand maneuvers at VLF frequency of 0.05 Hz, large oscillatory changes in BP and CBFV (TCD) were generated. Increase in oscillations in BP and TCD led to an increase in coherence in the VLF range and improved estimations of Cross Wavelet phase analysis. These findings showed that the large magnitude oscillations in BP and TCD induced during repeated sit-stand maneuvers not only provided strong and physiologically relevant hemodynamics perturbations, but also led to improved estimation of Cross Wavelet analysis of dynamic cerebral autoregulation at the very low frequencies. Compared with the spontaneous oscillations at baseline, coherence between BP and TCD was increased by these maneuvers. Large oscillations in BP at VLF frequency range may be compounded by cardiovascular resonance in response to external perturbations to BP [23].

The frequency of 0.05 Hz of repeated sit-stand maneuvers in this study is close to the baroreflex resonance frequencies observed in humans. The frequencies were selected around 0.05 Hz (10/10 s maneuver) and around 0.1 Hz range for analysis

because these are the frequencies where dynamic Cerebral Autoregulation (dCA) is active and repeated maneuvers [23,24] had been successful in inducing large oscillations with increased coherence at these frequencies. Indeed, repeated sit-stand maneuvers effectively induced oscillations at the intended frequencies and led to increased coherence.

In the high frequency range, the variability of repeated dCA assessments are expected to be high due to the variability in the cardiac cycle, which can significantly influence the assessment of dCA. In addition, above 0.2 Hz values of phase reach zero indicating that dCA is absent, leading to the dependency of TCD on BP, which has a high day-to-day variability. In the very low frequency range, changes in CBF are to a larger extent determined by factors outside BP [6]. However, if this was the case, reproducibility should have been improved for the repeated sit-stand maneuvers since these led to increased coherence between BP and CBF. This data suggests that with aging, autoregulation is well maintained up to frequencies of 0.1 Hz and our results of the Cross Wavelet analysis of the spontaneous oscillations at baseline are in accordance with the literature on dCA in healthy young and old subjects.

Generally, the sit-to-stand and the thigh-cuff techniques can both be used to assess cerebral autoregulation by inducing a transient drop in blood pressure and monitoring the cerebral blood flow response to this transient fall in cerebral perfusion pressure. But in this study sit-stand technique is used to assess cerebral autoregulation as these squat-stand maneuvers or thigh-cuff techniques may not be suitable and feasible in many (frail) older patients. For this reason, a less obtrusive technique is used to induce enhanced hemodynamic oscillations. Additionally, the sit-stand maneuvers causes a larger drop in TCD than thigh cuff deflation [25]. Moreover, we believe that these repeated sit-stand maneuvers would be much less strenuous and, therefore, more

widely applicable in older subjects than other repeated maneuvers that had been tested to date.

The active sit-to-stand procedure is known to be associated with an immediate increase in heart rate, which causes a pronounced increase in cardiac output [26] and a simultaneous fall in systemic vascular resistance, resulting in a transient fall in arterial BP. Therefore, the cause of the transient fall in arterial BP is a temporal mismatch between cardiac output (rate of blood volume entering the arterial vasculature) and vascular resistance (rate of blood volume leaving the arterial vasculature). Studies have shown that this mismatch results from a reduction in peripheral resistance [26] and not cardiac output. Active rising leads to a decrease in vascular resistance attributed to vasodilation in the working muscles through local mechanisms. This vasodilation peaks at 4 s and then returns to normal over the next 10–20 s [26]. In addition, standing up causes an initial increase in venous return through the effects of contraction of the leg and abdominal muscles. The consequent sudden increase in right arterial pressure activates cardiopulmonary receptors, resulting in a decrease in systemic sympathetic vasoconstrictor tone and total systemic vascular resistance lasting 6–8 s.

Estimates of dynamic Cerebral Autoregulation (dCA) in aging are based on the spontaneous oscillations. Using these spontaneous changes, an intact dCA is characterized by a high pass filter, i.e., phase decreases and gain increases with higher frequency oscillations [13]. Consistent with this model, Lipsitz et al. using measurements of spontaneous oscillations, observed larger phase shifts and lower gain in the low-frequency oscillations (0.04–0.15 Hz) compared with the high frequency oscillations (0.15–0.40) in 10 old subjects aged 72 (SD 3) years [27]. Thus our study provides a robust confirmation of these previous observations by Lipsitz et al. that dCA acts as a high pass filter over three established frequency ranges in community-dwelling (very) old,

indicating that dCA remains intact with aging [28]. In addition, the values of phase shift in the HF range reach approximately zero, which indicates that the TCD oscillations passively follow those of BP and that dCA is no longer active in the frequencies 0.2 Hz in both young [29] and (very) old subjects.

A cross-spectrum can be used to determine whether two processes result in oscillations within the same frequency region. The cross spectrum obtained from the Fourier transforms of an entire time series is uninformative, and a true cross spectrum must be estimated by windowing and averaging [30]. The continuous wavelet transform, which enables logarithmic frequency resolution, rather than the windowed Fourier, approach to coherence was used because it offers a more intuitive visualization of the time-frequency behaviour [30]. In this study, Cross Wavelet analysis has been used to analyze relationships between oscillations in blood flow, blood pressure and oxy-Deoxy haemoglobin within certain frequency ranges.

For biological signals that contain time-varying characteristic frequencies spread over a wide range, the use of adjustable windows should be considered mandatory. By its definition, the wavelet transform provides windows of adjustable length and, therefore, meets the mathematical requirements of a time-frequency analysis with logarithmic resolution.

Thus wavelet transform (time-frequency analysis) is used to compute phase and coherence to find out relationships between different parameters (systemic and hemodynamic) under baseline and repeated sit-stand maneuvers.

4.1 Wavelet Phase and Coherence

4.1.1 BP vs. TCD dynamic relationship on young and older subjects.

The magnitude of changes in BP and TCD induced by these repeated sit-stand maneuvers are much larger than those of baseline (spontaneous) oscillations and resembles the changes observed in daily life e.g., in conditions of orthostatic hypotension, post prandial hypotension, or carotid sinus syndrome. This enhances the clinical significance of this new autoregulation test, as the autoregulatory system is challenged with changes in BP that must be handled by older subjects in real life.

Phase shifts quantify the displacement of TCD oscillations relative to those of BP. Because changes in TCD recover faster than changes in BP, TCD oscillations appear to lead BP oscillations, which are indicated by a positive phase shift. Coherence, tests the linearity of the relation between BP and TCD oscillations. Since coherence approaching zero may indicate no relationship between the signals, severe extraneous noise in the signals, or a non-linear relationship, a value of 0.4 is considered the lower limit where transfer function estimates can be calculated with confidence.¹³ By convention, therefore, data with coherence <0.4 are excluded from analysis in most published studies. In this study, we will present data both with and without exclusion of coherence <0.4 .

Decrease in phase with increase in frequency for BP vs. TCD oscillations, confirmed observations based on spontaneous oscillations under resting conditions that phase shift is larger at the LF than the VLF frequencies. Phase for induced oscillations (i.e. at repeated sit-stand activity) at the VLF range [young: -0.86 radians (SD 0.16), old: -0.79 radians (SD 0.16)] was slightly lower than that from spontaneous oscillations [young: -1.06 radians (SD 0.58), old: -0.83 radians (SD 0.49)]. However, this difference is not

statistically significant. In addition, the improved signal-to-noise ratio may lead to improved accuracy of phase estimation at the VLF for induced oscillations.

The oscillations of TCD do not occur simultaneous to those of BP. Changes in TCD recover faster than changes in BP, which causes a displacement of TCD relative to BP in such a manner that TCD oscillations appear to lead BP oscillations. This is interpreted as intact dynamic Cerebral autoregulation. In relation to BP, this phase shift is mathematically negative.

The wavelet coherence function, tests the linearity of the relation between input and output. Coherence approaching unity in a specific frequency range suggests a linear relationship in this domain, whereas coherence approximating zero may indicate no relationship between the signals. However, a low coherence could also indicate severe extraneous noise in the signals. Therefore, for the calculation of phase shifts and gain values, thresholds of coherence of > 0.4 or > 0.5 have been used by most researchers. Conversely, low coherence can also be an expression of the nonlinear qualities of dCA and the validity of using these cut-off and maximum points is debatable. A solution to this limitation is to induce oscillatory changes in BP and TCD. These enlarge the power of the oscillations and thereby the coherence of the wavelet function.

Decrease in phase with increase in gain from VLF to HF range (Figure. 3-8) is consistent with the characteristics of a typical first-order high-pass filter, these observations indicate the presence of high-order regulatory mechanisms for cerebral hemodynamics.

The results of this study for healthy subjects are in agreement with the results of Latkaet al (2005) who investigated synchronization between BP and TCD-measured middle cerebral artery blood flow velocity using complex Morlet wavelets for ten healthy

young subjects and observed significantly reduced circular phase variance around LF and HF range.

In healthy aged subjects, dynamic cerebral autoregulation is preserved during induced drops in BP and during spontaneous oscillations in BP in the low frequency range (0.07 - 0.20 Hz). In the high frequency range (> 0.15 Hz), dynamic cerebral autoregulation is less efficient in both young and older people. This is in agreement with the concept that the relationship between BP and TCD can be expressed by transfer function analysis using a high-pass filter model.

It is well known that the standard deviation of heart rate decreases significantly with age. Reduced variability of heart rate with aging might have contributed to greater coherence within the corresponding cardiac interval. Cerebral Autoregulation is a high-pass filter that facilitates the transmission of BP changes to TCD and filters gradual BP changes [29]. The regulation of HbO is effective in the low frequency range of BP fluctuations but not in the high-frequency range because of the time delay required to initiate cerebrovascular adaptations to the changes in perfusion pressure.

4.1.2 TCD vs. HbO dynamic relationship on young and older subjects.

Spontaneous oscillations in HbO were detected in the very low and low frequency range, where also spontaneous variability in BP and TCD can be found [31]. This study shows that by using repeated sit-stand maneuvers, the dynamic CBF-brain tissue oxygenation relation can be assessed using cross wavelet analysis with a high coherence function (0.4) between these variables. It shows that how changes in CBF are transmitted to changes in brain tissue oxygenation by increased wavelet transform gain and phase at VLF range between changes in CBF velocity and HbO signal.

The repeated sit-stand maneuvers induced large oscillations in HbO that mirrored those in BP and TCD. The data indicate that oscillatory HbO changes in this

very low frequency range are related to the oscillations in TCD, which in turn are induced by oscillations in systemic BP. Taken together, the relationship between BP, TCD and HbO during repeated sit-stand maneuvers supports the notion that upstream oscillations in CBF induced by changes in BP contribute importantly to the downstream brain tissue level oscillations in HbO.

The dynamic relation between oscillations in TCD and HbO may reflect a regulatory mechanism to maintain brain tissue oxygenation homeostasis [32]. The investigation of the relationship between spontaneous oscillations in TCD and HbO using transfer function analysis suffers from the weakness and nonstationarity of the HbO measurement under resting conditions [32], but this weakness is removed in this study by using cross wavelet analysis technique. The repeated sit-stand maneuvers in this study induced large oscillations in BP, TCD, and HbO and enhanced coherence between TCD - HbO and therefore improve the reliability of the cross wavelet analysis. Further, the enhanced oscillations of HbO in response to changes in CBF may lead to local hypoxic changes in the brain. HbO oscillations seem to follow those of TCD (Figure 3-10) for both young and older subjects. Therefore, the phase difference between these variables may reflect a transit time between flow in supplying brain arteries and HbO. A larger phase lag between TCD and HbO is identified at the very low frequency range, but not in the low frequency (0.1 Hz). Because HbO is a correlate of local blood flow, this might point to a differential transfer of central blood flow to local blood flow and to local cerebral oxygenation. Whether this is due to differences in active regulation mechanisms or due to differences in the passive properties of the cerebral vasculature is not clear [33].

4.1.3 Study Limitation:

TCD measures changes in CBF based on the assumption that an insonated cerebral artery does not change or varies only slightly in diameter during measurements. Flow velocity in the MCA (middle cerebral artery) is determined by CBF and by the diameter of the MCA. Therefore, changes in CBFV reflect changes in CBF only if the MCA diameter is constant. During acute, moderate changes in BP, MCA diameter showed 4% change [24]. This suggests that small changes in MCA diameter cannot be excluded. This would have the following effects on our data. Vasoconstriction during an increase in BP overestimates the associated rise in CBF. Conversely, vasodilatation induced by a decrease in BP overestimates the reduction in CBF. Collectively, these effects, if they did occur, would overestimate wavelet function gain but would not affect phase, as this parameter is not affected by the amplitude but by the timing of the oscillations.

4.2 Conclusion

Thus from the results it can be seen that there is almost no significant statistical difference between (healthy) young and older subjects during baseline and repeated sit-stand activity. Using Wavelet coherence transform, circular phase shows that TCD leads BP, HbO and TOI; BP leads HbO and TOI and Hb leads TCD and BP. Thus it can be seen that during sit-stand activity the blood flow increases from macrocirculation to microcirculation following BP and then HbO and TOI. At VLF range (frequency at which repeated sit-stand activity is performed-0.05Hz) there is significant difference in young subjects than older subjects in circular phase, as the older subjects have stiff arteries, so the change in phase is low.

This study succeeded in inducing high-amplitude oscillations in the low frequencies, in combination with high coherence, thereby allowing confident comparisons

of the behavior of dynamic cerebral autoregulation in low vs. high frequencies. The magnitude of these hemodynamics changes as well as the maneuvers through which they are induced arguably are representative of the daily physiological challenges put to cerebral autoregulation

We conclude that addition of these maneuvers to an analysis based on spontaneous oscillations enhances the information obtained from Cross Wavelet analysis and may be an important step toward its translation and implementation in clinical medicine where patients are able to perform these maneuver.

Appendix A
Circular Statistics

Circular Mean and Circular Statistics

Due to the nature of the angular data, a subfield of statistics called circular statistics, has been applied for data analysis on an angular scale. On this scale, in contrast to a linear scale, there is not designated zero, and designation of high and low values is arbitrary [34]. These fascinating analyses find applications in different fields of science as diverse as engineering and physics such as geosciences [35], agricultural sciences (Aradottir, Robertson, Moore 1997) and psychology (Kubiak and Jonas 2007).

The circular nature of the angular data prevents the use of commonly used statistical techniques, as these would return misleading results that may result in wrong conclusions. The following techniques have been used to calculate mean, standard deviation and test of hypothesis, essential parameters to draw statistical meaningful conclusion.

Circular mean: the circular mean of a sample cannot be simply computed by averaging the data points. As an example, consider the following three angular measurements: 10°, 30° and 350°. The “linear” mean would yield 130°, but obviously the data points toward 0°. This simple example shows why the commonly applied statistical techniques fail when applied to angular data. Instead, in circular statistic, directions are first transformed into 2-D unit vectors:

$$R = \left\| \bar{r} \right\| \quad \text{A 1}$$

and the closer it is to 1 the more the circular probability distribution function will be peaked around the mean angular value. Based on this observation, the circular variance is closely related to the length of R by the following relationship (Berens 2009):

$$S = 1 - R \quad \text{A 2}$$

A first look at Equation (5.6) shows that, in contrast with the linear variance, the circular variance ranges between 0-1 and still, it is indicative of the data spread.

For example, if all data point in the same direction, $R=1$ and $\neq 0$. The standard deviation is defined as:

$$s = \sqrt{2(1-R)}$$

A 3

and lies in the interval $0-\sqrt{2}$ [34].

Appendix B

Relation of TCD and BP with TOI

Wavelet Phase and Coherence for TCD-TOI oscillations

The Figure below shows the Wavelet phase shift, coherence and gain for TCD and TOI for baseline and sit-stand maneuvers at VLF, LF and HF for young and elderly subjects. In this figure 3.2.d, we can see that there is significant phase shift at VLF range between young and older subject during sit-stand for TCD-Hb. The positive value of phase in the frequency range (0.045-0.3Hz) indicates changes in TCD leads changes in TOI. Wavelet phase shift increases, for TCD-TOI, with increase in frequency, for young subjects at VLF (0.3 ± 0.4) and HF (1.83 ± 0.8) and for older subjects at VLF (1.2 ± 0.8) and HF (2.12 ± 1.0) during sit-stand activity. Wavelet coherence is high and shows significant difference between young and older adults at baseline and sit-stand activity at VLF ($p < 0.005$) and LF ($p < 0.005$) range. Coherence values decrease as frequency increases.

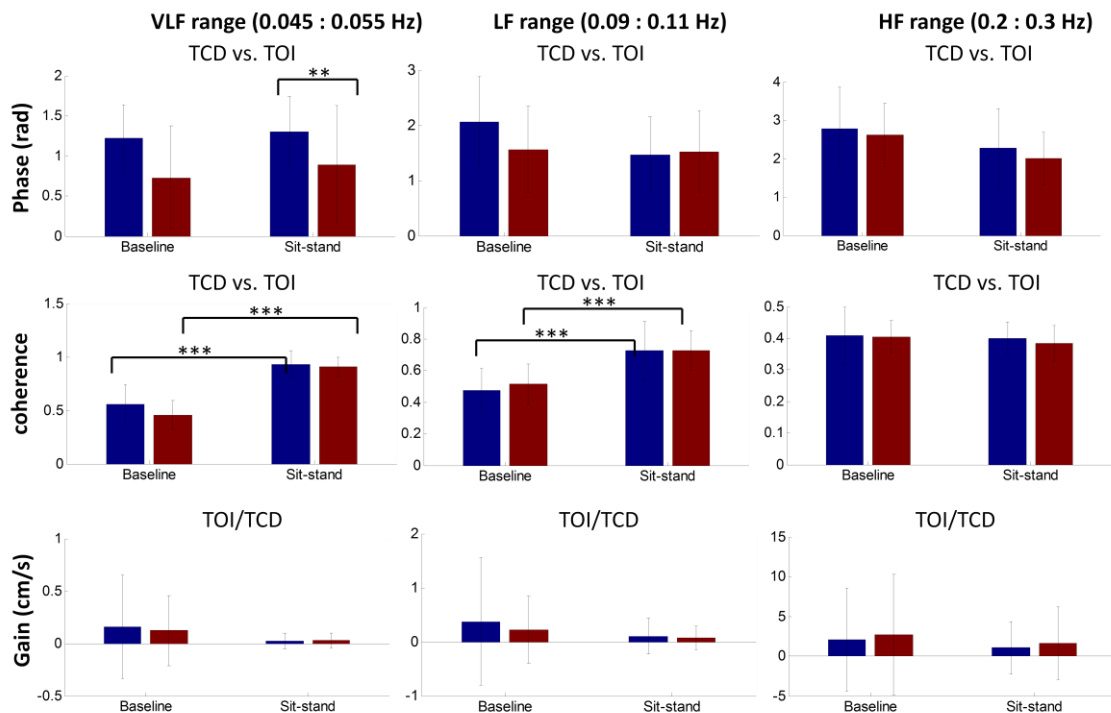


Figure A 1 group average bar plots of Wavelet phase (top), coherence (middle) for TCD and tissue oxygenation index for young (red) and older (blue) subjects. (* $p < 0.05$, ** $p < 0.01$, *** $p < 0.001$).

References

1. M. Wolf, M. Ferrari and V. Quaresima, "Progress of near-infrared spectroscopy and topography for brain and muscle clinical applications," *J Biomed Opt* **12**, 062104 (2007).
2. H. Owen-Reece, M. Smith and C. E. Elwell, "Near infrared spectroscopy," *British journal of* (1999).
3. G. Naulaers, "Non-invasive measurement of the neonatal cerebral and splanchnic circulation by near-infrared spectroscopy," (2003).
4. K. D. Liem and G. Greisen, "Monitoring of cerebral haemodynamics in newborn infants," *Early human development* (2010).
5. G. Greisen, "Autoregulation of cerebral blood flow in newborn babies," *Early human development* (2005).
6. R. B. Panerai, S. T. Deverson, P. Mahony, P. Hayes and D. H. Evans, "Effects of CO₂ on dynamic cerebral autoregulation measurement," *Physiol Meas* **20**, 265-75 (1999).
7. P. N. Ainslie and J. Duffin, "Integration of cerebrovascular CO₂ reactivity and chemoreflex control of breathing: mechanisms of regulation, measurement, and interpretation," *Am. J. Physiol. Regul. Integr. Comp. Physiol* **296**, R1473-95 (2009).
8. E. Bor-Seng-Shu, W. S. Kita, E. G. Figueiredo, W. S. Paiva, E. T. Fonoff, M. J. Teixeira and R. B. Panerai, "Cerebral hemodynamics: concepts of clinical importance," *Arq Neuropsiquiatr* **70**, 352-6 (2012).
9. V. Marmarelis, D. Shin and R. Zhang, "Linear and nonlinear modeling of cerebral flow autoregulation using principal dynamic modes," *Open Biomed Eng J* **6**, 42-55 (2012).

10. N. A. LASSEN, "Cerebral blood flow and oxygen consumption in man," *Physiol. Rev* **39**, 183-238 (1959).
11. R. Aaslid, K. F. Lindegaard, W. Sorteberg and H. Nornes, "Cerebral autoregulation dynamics in humans," *Stroke* (1989).
12. A. H. van Beek, J. Lagro, M. G. Olde-Rikkert, R. Zhang and J. A. Claassen, "Oscillations in cerebral blood flow and cortical oxygenation in Alzheimer's disease," *Neurobiol. Aging* **33**, 428.e21-31 (2012).
13. A. H. van Beek, M. G. Olde Rikkert, J. W. Pasman, M. T. Hopman and J. A. Claassen, "Dynamic cerebral autoregulation in the old using a repeated sit-stand maneuver," *Ultrasound Med Biol* **36**, 192-201 (2010).
14. A. Stefanovska, M. Bracic and H. D. Kvernmo, "Wavelet analysis of oscillations in the peripheral blood circulation measured by laser Doppler technique," *IEEE Trans Biomed Eng* **46**, 1230-9 (1999).
15. A. Bandrivskyy, A. Bernjak and P. McClintock, "Wavelet phase coherence analysis: application to skin temperature and blood flow," : an international journal (2004).
16. T. Tarumi, M. A. Khan, J. Liu, B. M. Tseng and R. Parker, "Cerebral hemodynamics in normal aging: central artery stiffness, wave reflection, and pressure pulsatility," *Cerebral Blood Flow &* (2014).
17. L. M. Van Bortel, S. Laurent, P. Boutouyrie, P. Chowienczyk, J. K. Cruickshank, T. De Backer, J. Filipovsky, S. Huybrechts, F. U. Mattace-Raso, A. D. Protogerou and G. Schillaci, "Expert consensus document on the measurement of aortic stiffness in daily practice using carotid-femoral pulse wave velocity," *J. Hypertens* **30**, 445-8 (2012).

18. S. Laurent, J. Cockcroft, L. Van Bortel, P. Boutouyrie, C. Giannattasio, D. Hayoz, B. Pannier, C. Vlachopoulos, I. Wilkinson, H. Struijker-Boudier and H. Struijker-Boudier, "Expert consensus document on arterial stiffness: methodological issues and clinical applications," *Eur. Heart J* **27**, 2588-605 (2006).
19. C. Torrence and G. P. Compo, "A practical guide to wavelet analysis," the American Meteorological society (1998).
20. A. Grinsted and J. C. Moore, "Application of the cross wavelet transform and wavelet coherence to geophysical time series," in *geophysics* (2004).
21. A. Grinsted and J. C. Moore, "Application of the cross wavelet transform and wavelet coherence to geophysical time series," *Nonlinear* (2004).
22. R. R. Diehl, D. Linden, D. Lücke and P. Berlit, "Phase relationship between cerebral blood flow velocity and blood pressure. A clinical test of autoregulation," *Stroke* **26**, 1801-4 (1995).
23. J. W. Hamner, M. A. Cohen, S. Mukai, L. A. Lipsitz and J. A. Taylor, "Spectral indices of human cerebral blood flow control: responses to augmented blood pressure oscillations," *J. Physiol. (Lond.)* **559**, 965-73 (2004).
24. J. A. H. R. Claassen and B. D. Levine, "Dynamic cerebral autoregulation during repeated squat-stand maneuvers," *Journal of Applied* (2009).
25. F. A. Sorond, J. M. Serrador, R. N. Jones, M. L. Shaffer and L. A. Lipsitz, "The sit-to-stand technique for the measurement of dynamic cerebral autoregulation," *Ultrasound Med Biol* **35**, 21-9 (2009).
26. W. Wieling, C. T. Krediet, N. van Dijk, M. Linzer and M. E. Tschakovsky, "Initial orthostatic hypotension: review of a forgotten condition," *Clin. Sci* **112**, 157-65 (2007).

27. L. A. Lipsitz, S. Mukai, J. Hamner, M. Gagnon and V. Babikian, "Dynamic regulation of middle cerebral artery blood flow velocity in aging and hypertension," *Stroke* **31**, 1897-903 (2000).
28. L. A. Lipsitz, S. Mukai, J. Hamner, M. Gagnon and V. Babikian, "Dynamic regulation of middle cerebral artery blood flow velocity in aging and hypertension," *Stroke* **31**, 1897-903 (2000).
29. R. Zhang, J. H. Zuckerman and C. A. Giller, "Transfer function analysis of dynamic cerebral autoregulation in humans," *American Journal of (1998)*.
30. L. W. Sheppard, A. Stefanovska and P. V. McClintock, "Testing for time-localized coherence in bivariate data," *Phys Rev E Stat Nonlin Soft Matter Phys* **85**, 046205 (2012).
31. H. Obrig, M. Neufang, R. Wenzel, M. Kohl, J. Steinbrink, K. Einhupl and A. Villringer, "Spontaneous low frequency oscillations of cerebral hemodynamics and metabolism in human adults," *Neuroimage* **12**, 623-39 (2000).
32. A. B. Rowley, S. J. Payne, I. Tachtsidis, M. J. Ebden, J. P. Whiteley, D. J. Gavaghan, L. Tarassenko, M. Smith, C. E. Elwell and D. T. Delpy, "Synchronization between arterial blood pressure and cerebral oxyhaemoglobin concentration investigated by wavelet cross-correlation," *Physiol Meas* **28**, 161-73 (2007).
33. J. B. Mandeville, J. J. Marota, C. Ayata, G. Zaharchuk, M. A. Moskowitz, B. R. Rosen and R. M. Weisskoff, "Evidence of a cerebrovascular postarteriole windkessel with delayed compliance," *J. Cereb. Blood Flow Metab* **19**, 679-89 (1999).
34. P. Berens, "CircStat: a MATLAB toolbox for circular statistics," *J Stat Softw* (2009).

35. J. A. Bowers, I. D. Morton and G. I. Mould, "Directional statistics of the wind and waves," Applied Ocean Research (2000).

Biographical Information

Mrunmayee Gandhi was born in Pune, Maharashtra, India on March 24, 1990. In May 2012, she received the B. Tech degree in Instrumentation and Control engineering from the Vishwakarma Institute of Technology, in Pune, India. In August 2012, she joined University of Texas at Arlington for the Master's degree program of Bioengineering. She had research interest in bio-imaging and hence, she started working in Dr. Hanli Liu's lab as a research assistant at the University of Texas at Arlington, USA. In the lab, she worked on many projects related to brain imaging. Her research work during her Master Thesis was focused on signal processing for cerebral hemodynamics monitoring using cross wavelet analysis. The future goal is to find out the effects of cerebral hemodynamic variables and systemic variables on severe brain injuries.